scientific reports

Check for updates

OPEN

Glucose impacts onto the reciprocal reprogramming between mammary adipocytes and cancer cells

Maria Rosaria Ambrosio[1]✉, Michiel Adriaens[2], Kasper Derks[3], Teresa Migliaccio[4], Valerio Costa[5], Domenico Liguoro[1], Simona Cataldi[5], Vittoria D'Esposito[1], Giovanni Maneli[4], Rita Bassolino[4], Simone Di Paola[1], Marinella Pirozzi[1], Fabrizio Schonauer[6], Francesco D'Andrea[6], Francesco Beguinot[1,4], Ilja Arts[2] & Pietro Formisano[1,4]✉

An established hallmark of cancer cells is metabolic reprogramming, largely consisting in the exacerbated glucose uptake. Adipocytes in the tumor microenvironment contribute toward breast cancer (BC) progression and are highly responsive to metabolic fluctuations. Metabolic conditions characterizing obesity and/or diabetes associate with increased BC incidence and mortality. To explore BC-adipocytes interaction and define the impact of glucose in such dialogue, Mammary Adipose-derived Mesenchymal Stem Cells (MAd-MSCs) were differentiated into adipocytes and co-cultured with ER$^+$ BC cells while exposed to glucose concentration resembling hyperglycemia or normoglycemia in humans (25mM or 5.5mM). The transcriptome of both cell types in co-culture as in mono-culture was profiled by RNA-Seq to define the impact of adipocytes on BC cells and *viceversa* (i), the action of glucose on BC cells, adipocytes (ii) and their crosstalk (iii). Noteworthy, we provided evidence that co-culture with adipocytes in a glucose-rich environment determined a re-program of BC cell transcriptome driving lipid accumulation, a hallmark of BC aggressiveness, promoting stem-like properties and reducing Tamoxifen responsiveness. Moreover, our data point out to a transcriptional effect through which BC cells induce adipocytes de-lipidation, paralleled by pluripotency gain, as source of lipids when glucose lowering occurs. Thus, modulating plasticity of peri-tumoral adipocytes may represent a key point for halting BC progression in metabolically unbalanced patients.

Keywords Tumor Microenvironment, Mammary Adipocytes, Breast Cancer, Glucose, Transcriptional signatures, Adipogenesis

The concurrence of obesity and type 2 diabetes (T2D) pandemics with the growing burden of cancer globally justifies the interest in defining the biological relationship between these pathological conditions[1,2]. Breast cancer (BC) is the most common female malignant neoplasia and the first cause of cancer death in women worldwide[3]. In BC, the excess of bodyweight is a negative prognostic factor independently to menopause status and T2D is associated with more aggressive cancer phenotype[4,5].

A firmly established hallmark of cancer cells is a metabolic reprogramming consisting in the activation of pathways to support proliferation, to help the adaptation to oxidative stress, and to provide energy for biomass synthesis, migration and invasion[6]. A pivotal adaptive event in tumor metabolism is the so-called "Warburg effect" and consists of an exacerbated glucose uptake and glycolysis utilization leading to increased lactate production[7]. Functionally dependent on glucose catabolic pathways but commonly disregarded in the past, alterations in lipid- and cholesterol-associated pathways encountered in tumors are now well recognized and more frequently described[8]. Thus, there is consensus that cancer cells display metabolic reprogramming

[1]Institute of Experimental Endocrinology and Oncology "G. Salvatore", National Council of Research (IEOS-CNR), Naples, Italy. [2]Maastricht Center for Systems Biology (MaCSBio), Maastricht University, Maastricht, The Netherlands. [3]Department of Clinical Genetics, Maastricht University Medical Center, Maastricht, The Netherlands. [4]Department of Translational Medicine (DiSMeT), University of Naples "Federico II", Naples, Italy. [5]Institute of Genetics and Biophysics "A. Buzzati Traverso", National Council of Research (IGB-CNR), Naples, Italy. [6]Department of Public Health, University of Naples "Federico II", Naples, Italy. ✉email: mariarosaria.ambrosio@cnr.it; fpietro@unina.it

compared to healthy cells, related not only to the Warburg effect but also to de-novo synthesis because of their strong lipid and cholesterol avidity[9]. Excessive lipids and cholesterol in cancer cells are stored in lipid droplets (LDs); indeed, high LDs and stored-cholesteryl ester content in tumors are now considered as hallmarks of cancer aggressiveness and chemotherapy resistance[8,9].

In this *scenario*, tumor acts as parasite sequestering metabolic elements - via stimulation of catabolic pathways - that are utilized as substrates for anaerobic metabolism in cancer cells[10]. There is now cumulative evidence that cells immediately adjacent to a tumor are not only passive structural elements but also active actors in tumor progression[3,11]. Thus, accordingly with the widely accepted idea that, during tumor progression, the tumor cell "seed" co- evolves with the surrounding microenvironment "soil", tumor-associated stroma is a prerequisite for tumor cell invasion and metastasis[12,13]. In this context, tumor cells can efficiently recruit stromal cells - fibroblast, pericytes, mesenchymal stem cells, macrophages, immune cells and adipocytes - by secreting stimulatory growth factors, chemokines and cytokines; in turn, these non-cancerous host cells secrete a plethora of mediators and growth factors that support tumor progression[14].

In the highly vicious cycle orchestrated by cancer cells, adipocytes participate acting as endocrine cells, in contrast to the previous perception of adipocytes as adjacent, static cells next to tumor; meanwhile, cancer cells dramatically impact on surrounding adipocytes that exhibit an altered phenotype and specific biological features[13,15]. In breast, an interaction between epithelial cells and adipocytes exists in normal tissue as well as in cancer; the intimate and bi-directional interaction with adjacent epithelium is one of the hallmarks of mammary adipocytes, suggesting that this dialog might persist in pathological conditions, including the whole process of cancer[16,17]. Adipocytes involved in BC progression are known as cancer-associated adipocytes (CAAs)[18]. CAAs form clusters of smaller-sized adipocytes - due to lipolysis, changes in lipid droplets and modifications of adipocyte-related basement membranes and extracellular matrix - that are present in the invasive front of BC[19]. Therefore, adipocytes represent a dynamic partner of BC cells; together they establish a reciprocal reprogramming that generates a dangerous duo that favors breast tumor progression[20–22].

Considering that T2D and obesity are now established risk factors for BC and tumor related mortality, one of the main consequences of adipocytes-cancer cells bi-directional communication concerns the prognosis of cancer in obese and/or diabetic patients[16]. It should be speculated that the contribution of adipocytes into tumor progression might be amplified in women affected by metabolic alterations, thus explaining, at least in part, the poor prognosis observed in such patients. Here, we analyzed the impact of glucose in the dialogue between BC cells and mammary adipocytes by simulating the reduction of glucose levels when an "hyperglycemic-like condition" occurs. Thus, MCF7 (ER^+, PR^+, $HER2^-$) BC cells and differentiated mammary adipocytes were co-cultured while exposed to basal 25mM glucose (High Glucose; HG) or shifted to 5.5mM glucose (Low Glucose; LG), mimicking hyperglycemia or normoglycemia in humans, respectively. Whole transcriptome of both cell types was profiled by RNA-Sequencing. Differential expression analysis highlighted that adipocytes and BC cells reciprocally reprogram their gene expression profiles either independently or dependently of glucose levels. We obtained evidence that adipocytes sustain BC aggressiveness by activating "adipogenesis-related" pathways, particularly in HG. On the other hand, a de-differentiation program is induced in adipocytes when co-cultured with BC cells, predominantly upon glucose lowering. Notably, we demonstrated that adipocytes in HG promote the ability of cancer cells to form mammospheres (i.e. stem-like properties) and reduce cell responsiveness to Tamoxifen both in 2D and in 3D systems.

Results

Evaluating the effect of glucose and adipocytes on MCF7 BC cell transcriptome

Transcript-level differential expression analysis of RNA-Seq data highlighted that co-culturing MCF7 with adipocytes caused a reshaping of cancer cell transcriptional profile. Data analysis revealed that (1) glucose lowering (HG-> LG) *per se* determined transcriptome changes in MCF7 (167 differentially expressed transcripts – DETs), (2) adipocytes modified MCF7 transcriptome both in HG (3496 DETs) and in LG (3032 DETs) (Figs. 1), (3) glucose levels affected the transcriptome of co-cultured cancer cells (1077 DETs in Co-Cultured $MCF7_{HG->LG}$ *vs* Co-cultured $MCF7_{HG}$; Table 1).

Based on the intersection of DETs (Fig. 1; p-val < 0.05) obtained from each comparison, 26 genes (59 transcripts) exclusively regulated by glucose in MCF7 were identified and reported in Supplementary Table S1. Other 13 genes (33 transcripts) were de-regulated in MCF7 upon glucose lowering also in presence of adipocytes (Fig. 1); among them, 12 genes displayed an opposite adipocyte *vs* glucose effect, while only for *OPTN* gene a potentially additive (adipocytes + glucose) effect was detected (Fig. 2).

Notably, 648 genes (1675 transcripts) were similarly up- or down-regulated (UP or DW, respectively) in MCF7 when co-cultured with adipocytes, both in LG and in HG (Fig. 1). Those with the greatest fold changes (adjp-val < 0.01) were reported in Supplementary Table S2). Nevertheless, glucose concentrations may affect the extent of adipocyte-elicited effects; *GATS* was the only gene DW-regulated in MCF7 co-cultured with adipocytes in LG while UP-regulated when cancer cells were co-cultured with adipocytes in HG (Fig. 3).

Finally, 777 genes (1746 transcripts) and 552 genes (1282 transcripts) were modulated in MCF7 by adipocytes exclusively in HG or LG, respectively (Fig. 1). Those with the greatest fold changes (adjp-val < 0.01) were reported in Tables 2 and 3, respectively. Pathway analysis revealed that most of DEGs in co-cultured BC cells, independently of glucose levels, were involved in focal adhesion, ECM organization and apoptosis processes thus suggesting a re-programming of cancer cells in terms of proliferation and motility when co-cultured with adipocytes; in addition, some genes were found involved in inflammatory cytokine signaling (i.e. IL-11 and IL-17). Noteworthy, a highly represented process among de-regulated pathways (Z-score higher than 1.5) in co-cultured BC cells was adipogenesis, also independently of glucose (Fig. 4).

Indeed, some DEGs in co-cultured BC cells encoded for miscellaneous factors, adipocyte secretory products and markers of fully differentiated adipocytes; such "adipogenesis-related" genes were differentially while

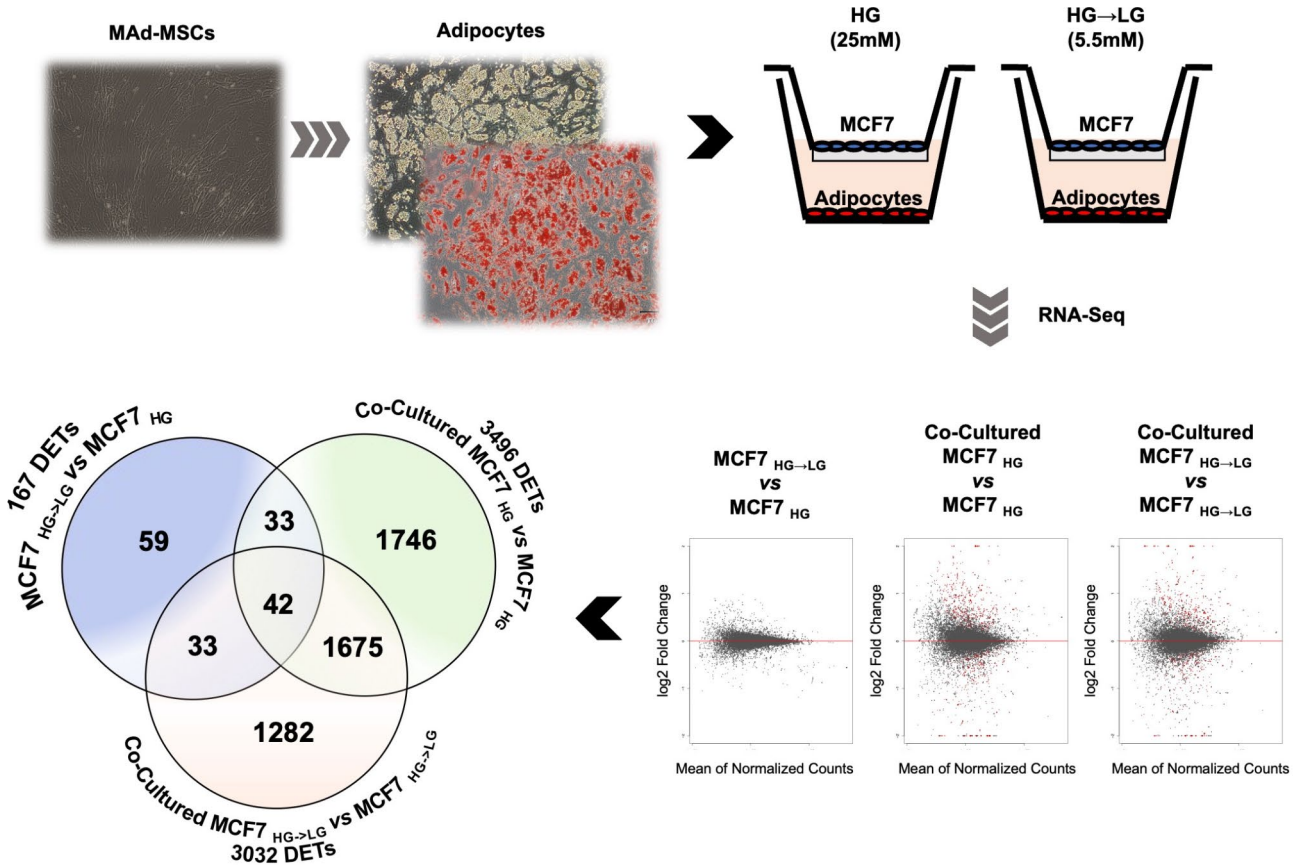

Figure 1. Effect of glucose and/or adipocytes on MCF7 BC cell transcriptome. Schematic representation of the experiment: Adipose-derived Mesenchymal Stem Cells (MAd-MSCs) were differentiated into mature adipocytes on the bottom chamber of a transwell system. At the 15th days of the differentiation process, MCF7 were seeded in the upper chamber of the system. BC cells were co-cultured with adipocytes for 4 days while exposed to basal 25mM glucose (High Glucose, HG; Co-Cultured MCF7 $_{HG}$) or shifted to 5.5mM glucose (Low Glucose, LG; Co-Cultured MCF7 $_{HG-> LG}$). In parallel, MCF7 were mono-cultured in basal HG (MCF7 $_{HG}$) or shifted to LG (MCF7 $_{HG-> LG}$). RNA samples from three independent experiments were obtained for RNA-Seq. Computational data analysis provided Differentially Expressed Transcripts (DETs; p-val < 0.05) from MCF7 $_{HG-> LG}$ vs. MCF7 $_{HG}$ (Glucose lowering), Co-Cultured MCF7 $_{HG}$ vs. MCF7 $_{HG}$ (Co-Culture with adipocytes in HG) and Co-Cultured MCF7 $_{HG-> LG}$ vs. MCF7 $_{HG-> LG}$ (Co-Culture with adipocytes in LG) comparisons. Unique or common DETs were discriminated by intersecting lists of DETs.

others were similarly regulated by adipocytes in presence of different glucose levels. Of note, transcription factors involved in preadipocyte to adipocyte transition, including *PPARG* and its regulators/cooperators, were differentially expressed in co-cultured BC cells. Moreover, many de-regulated genes are involved in PPARG signaling pathway and, particularly, in fatty acid metabolism (Fig. 5A-B). We also found that insulin receptor (InsR) levels were lower in HG compared to LG monocultures. However, InsR mRNA and protein levels were up-regulated when BC cells were co-cultured with adipocytes in HG (Fig. 5B-C and Supplementary Figure S1).

Evaluating the effect of glucose and breast cancer cells on adipocyte transcriptome

RNA-Sequencing revealed both glucose (2745 DETs) and BC cells (4931 DETs in HG and 1585 DETs in LG) affected the transcriptome of mammary adipocytes (Fig. 6) and that glucose lowering modulates gene expression profile of co-cultured adipocytes (194 DETs in Co-Cultured Adipo $_{HG-> LG}$ vs. Co-Cultured Adipo $_{HG}$; Table 4).

Based on the intersection of DETs (Fig. 6; p-val < 0.05) obtained from each comparison, 536 genes (997 transcripts) regulated by glucose were identified in mono-cultured mammary adipocytes. Those with the greatest fold change (adjp-val < 0.01) were reported in Supplementary Table S3. Moreover, 32 genes (49 transcripts) were de-regulated in adipocytes upon glucose lowering also in co-culture with MCF7 cells (Fig. 6) and displayed an opposite MCF7 glucose effect (Fig. 7).

Notably, 315 genes (782 transcripts), were similarly UP or DW regulated in adipocytes when co-cultured with MCF7 cells, both in LG and in HG (Fig. 6); nevertheless, glucose concentrations may affect the extent of MCF7-elicited effects (Supplementary Table S4). Finally, 1123 genes (2450 transcripts) and 339 genes (705 transcripts) in adipocytes were modulated by MCF7 cells exclusively in HG or LG, respectively (Fig. 6);those with the greatest fold changes (adjp-val < 0.01) were reported in Tables 5 and 6, respectively.

Gene symbol	Description	mRNA transcripts	log2 FC	*p*-val
NEDD9	Neural precursor cell expressed, developmentally down-regulated 9	NM_182966	1.40	2.98E-02
PTPRB	Protein tyrosine phosphatase, receptor type B	NM_001206971	1.28	3.72E-04
SOX9	SRY-box 9	NM_000346	1.17	2.40E-03
PTPRB	Protein tyrosine phosphatase, receptor type B	NM_002837 NM_001206972	1.13 1.11	1.21E-03 1.50E-03
ZNF285	Zinc finger protein 285	NM_001291490 NM_152354 NM_001291489 NM_001291488	1.08 1.05 1.05 1.05	9.81E-03 1.10E-02 1.10E-02 1.10E-02
PTPRB	Protein tyrosine phosphatase, receptor type B	NM_001109754 NM_001330204	1.01 1.00	2.94E-03 3.68E-03
CTSZ	Cathepsin Z	NM_001336	0.96	3.59E-03
C16orf45	Chromosome 16 open reading frame 45	NM_033201	0.94	2.88E-02
ATF3	Activating transcription factor 3	NM_001030287	0.94	3.59E-03
AK5	Adenylate kinase 5	NM_174858	0.93	2.12E-02
CHAC1	ChaC glutathione specific gamma-glutamylcyclotransferase 1	NM_001142776	0.93	4.38E-03
ATF3	Activating transcription factor 3	NM_001206484 NM_001206488	0.92 0.92	3.24E-03 3.08E-03
AK5	Adenylate kinase 5	NM_012093	0.91	2.65E-02
CHAC1	ChaC glutathione specific gamma-glutamylcyclotransferase 1	NM_024111	0.91	5.38E-03
TCAF2	TRPM8 channel associated factor 2	NM_001130026	0.91	3.73E-02
ATF3	Activating transcription factor 3	NM_001674 NM_001206486	0.89 0.74	3.91E-03 2.16E-02
APBB1	Amyloid beta precursor protein binding family B member 1	NM_001164 NM_145689	-0.76 -0.76	4.37E-04 3.94E-04
HDX	Highly divergent homeobox	NM_144657 NM_001177479	-0.95 -0.95	3.22E-03 3.22E-03
CDKN1C	Cyclin dependent kinase inhibitor 1 C	NM_001122631 NM_001122630 NM_000076	-0.96 -0.96 -0.96	1.87E-02 1.88E-02 1.91E-02
APBB1	Amyloid beta precursor protein binding family B member 1	NM_001257325 NM_001257323 NM_001257319 NM_001257326 NM_001257321 NM_001257320	-0.96 -0.96 -0.96 -0.97 -0.97 -0.99	3.26E-04 3.27E-04 3.28E-04 2.79E-04 2.79E-04 1.74E-04
HSD11B1L	Hydroxysteroid 11-beta dehydrogenase 1 like	NM_198705 NM_198708	-1.00 -1.01	5.70E-03 8.11E-03
HDX	Highly divergent homeobox	NM_001177478	-1.02	1.82E-03
HSD11B1L	Hydroxysteroid 11-beta dehydrogenase 1 like	NM_198706 NM_001267868 NM_001267869 NM_198707 NM_001267870	-1.03 -1.03 -1.03 -1.04 -1.05	6.67E-03 6.49E-03 5.06E-03 3.95E-03 6.73E-03
ARL4D	ADP ribosylation factor like GTPase 4D	NM_001661	-1.05	5.34E-03
CSF1	Colony stimulating factor 1	NM_172212	-1.08	2.05E-02
HSD11B1L	Hydroxysteroid 11-beta dehydrogenase 1 like	NM_001267871 NM_198533 NM_198704	-1.12 -1.15 -1.16	4.62E-03 5.19E-03 4.07E-03
CSF1	Colony stimulating factor 1	NM_172210	-1.20	1.30E-02
ARRDC4	Arrestin domain containing 4	NM_183376	-1.45	3.44E-06
TXNIP	Thioredoxin interacting protein	NM_006472 NM_001313972	-2.42 -2.42	6.04E-12 7.19E-12

Table 1. DETs in co-cultured MCF7 $_{HG-> LG}$*vs* co-cultured MCF7 $_{HG}$

Pathway analysis revealed that upon co-culture with BC cells most DEGs were related to glycolysis and gluconeogenesis processes independently of glucose levels. In addition, only in HG, genes involved in histone modification process were highly represented among pathways. TGF-beta signaling pathway, instead, is one of the most relevant components upon glucose lowering (Fig. 8).

Interestingly, mostly in LG, a de-regulation occurred both in pluripotency and in adipogenesis-related pathways (Fig. 9A). For instance, we found a down-regulation of PPARG mRNA and protein levels, paralleled by a de-regulation of genes able to promote the self-renewal (Fig. 9B-C).

The induction of adipocytes de-lipidation upon co-culture with BC cells in LG was further confirmed at morphological levels. As shown in Fig. 10, both Oil Red O and immunofluorescence analysis highlighted that,

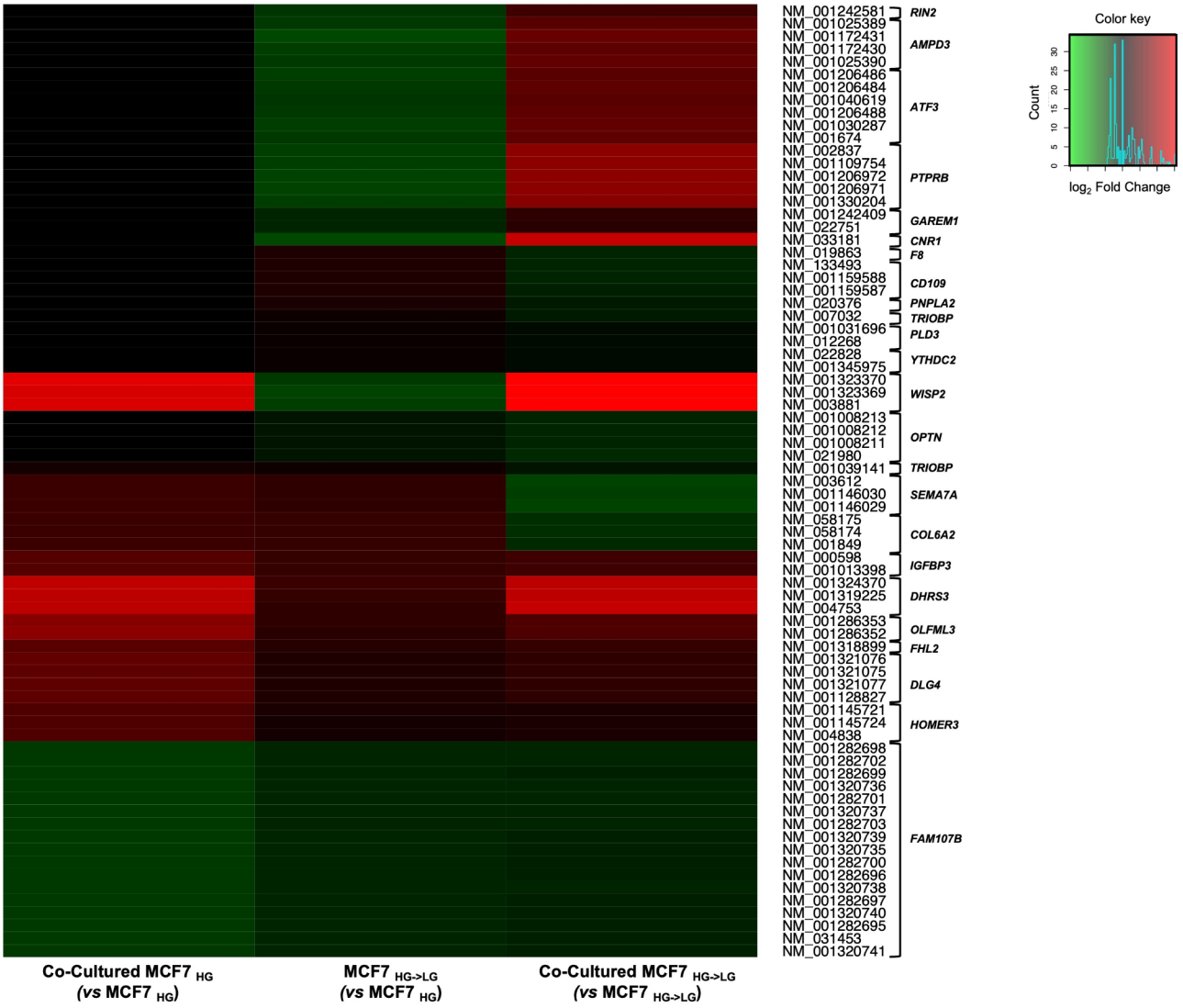

Figure 2. Commonly modulated genes by glucose and adipocytes in MCF7 BC cells. Normalized expression values of transcripts commonly modulated in MCF7 by adipocytes (Co-Cultured MCF7 $_{HG}$*vs* MCF7 $_{HG}$), glucose lowering (MCF7 $_{HG-> LG}$*vs* MCF7 $_{HG}$) and glucose lowering + adipocytes (Co-Cultured MCF7 $_{HG-> LG}$*vs*. MCF7 $_{HG-> LG}$).

while glucose lowering *per se* did not modify lipid accumulation (Supplementary Figure S1), BC induce the reduction of lipid droplets amount in adipocytes when co-cultured in LG environment (Fig. 10).

Effect of adipocytes on BC cell growth and Tamoxifen responsiveness

MCF7 from co-cultures in HG or LG (i.e. Co-Cultured MCF7 $_{HG}$ and Co-Cultured MCF7 $_{HG-> LG}$, respectively) were used to establish three-dimensional spheroids in presence and in absence of conditioned media from Co-Cultured Adipo $_{HG-> LG}$ and Co-Cultured Adipo $_{HG}$. We found that MCF7 from co-cultures in HG were able to form a 1.3-fold higher number of mammospheres, also characterized by about 40% increased diameter, compared to those from co-cultures in LG (Fig. 11A; $pval < 0.05$). To further assess the effect of adipocytes on BC cells, Tamoxifen responsiveness was investigated by treating MCF7 when co-cultured with adipocytes in HG or LG. As shown in Fig. 11B, Tamoxifen treatment did not induce cell death of MCF7 when co-cultured with adipocytes both in HG and in LG; interestingly, MCF7 viability was significantly higher in co-cultured than in monocultured cells in HG while not in LG (Fig. 11B; $pval < 0.01$). Thus, Tamoxifen effectiveness in 3D model exposed to HG was also assessed. As shown in Fig. 11C, cell viability of MCF7 spheroids obtained from co-cultures in HG - basically significantly higher than that of spheroids obtained from monocultured cells - was not affected by Tamoxifen treatment (Fig. 11C; $pval < 0.01$).

Evaluating the effect of glucose onto the interplay between BC cell lines and adipocytes

Adipogenic (*PPARG*, *CEBPB*, *CEBPD*, *FAS*, *PLIN2*, *LPIN2*, *INSR*) genes were also measured when BT474 (ER^+ HER^+ PR^-), SKBR3 (ER^- HER^+ PR^-) and MDA-MB231 (ER^- HER^- PR^-) cells were co-cultured with

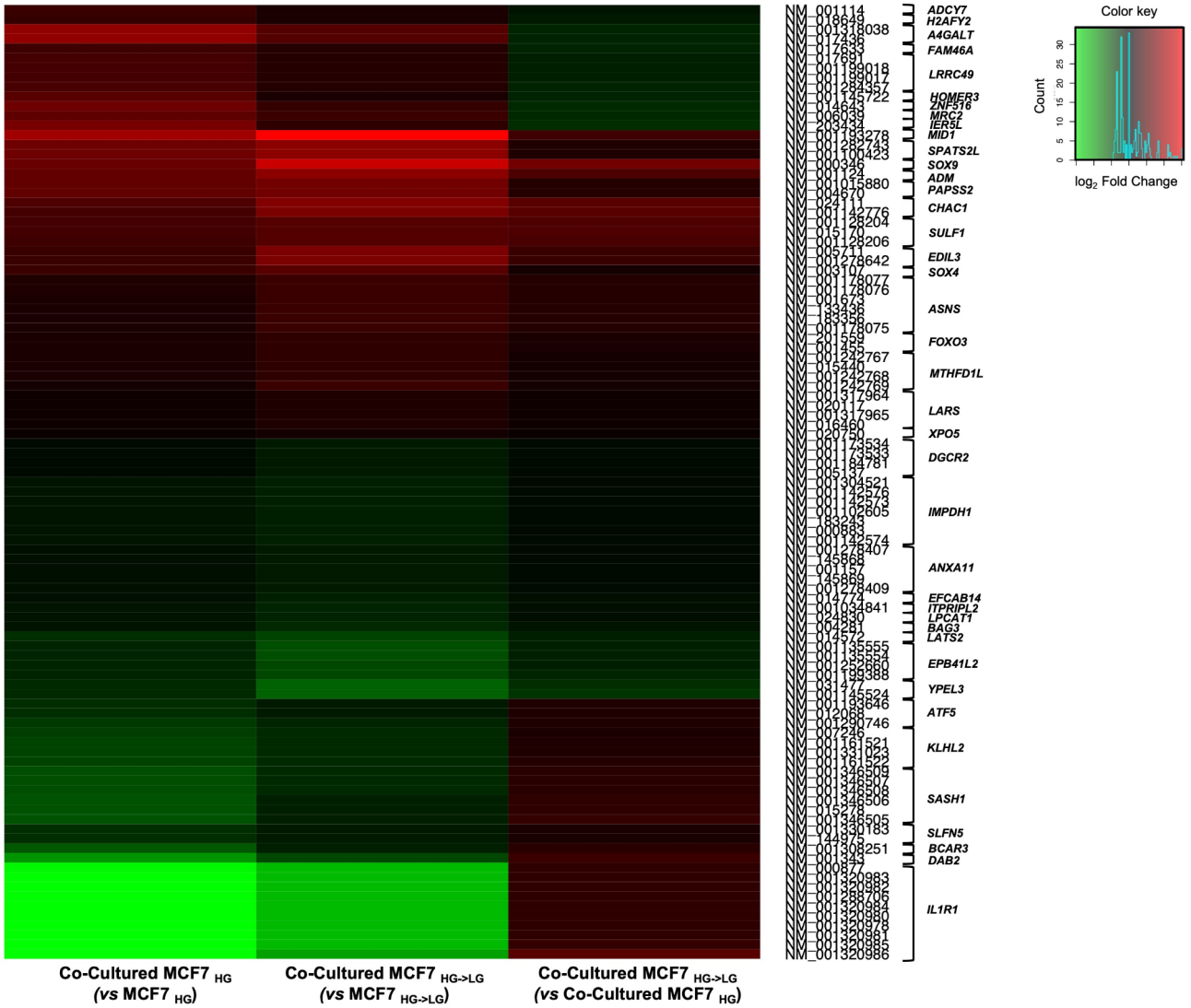

Figure 3. Glucose-dependent gene regulation by adipocytes in MCF7 BC cells. Normalized expression values of transcripts commonly modulated in MCF7 by adipocytes in HG (Co-Cultured MCF7 $_{HG}$*vs* MCF7 $_{HG}$) and in LG (Co-Cultured MCF7 $_{HG->LG}$*vs* MCF7 $_{HG->LG}$), also differentially expressed comparing co-cultured cells (Co-Cultured MCF7 $_{HG->LG}$*vs* Co-Cultured MCF7 $_{HG}$).

adipocytes under different glucose concentration. We observed only glucose-induced increase of *FAS* mRNA levels in SKBR3 cells co-cultured with adipocytes. Only slight modulation of the other genes was observed (Fig. 12). In adipocytes co-cultured with BT474, SKBR3 or MDA-MB231 under different glucose concentration, no changes in adipogenic and pluripotency genes (*AXIN*, *WNT5B*, *PPARG*, *CEBPA*, *OCT4*, *SOX2*, *NANOG*) as well as in lipid content were observed (Fig. 13).

Discussion

In the past few decades, global data highlight the exponential increase in the incidence of obesity, diabetes and cancer, and display evidence of association among them. Thus, it is mandatory that research concerning such biological links and clinical patient management for individuals suffering for these comorbidities need to be deeply understood[1].

Tumor microenvironment is a heterogeneous mixture of tumor cells and endogenous host stroma that co-evolve during the course of disease progression[23]. Breast is a fat-rich organ in which cancer cell progression is strongly regulated by the direct crosstalk with tumor-surrounding adipocytes[16]. The dialogue between adipocytes and BC cells within the tumor microenvironment leads to morphological and functional alterations of both cell types, which is gradually being recognized as an integral part of cancer development and progression[13].

Given that metabolic abnormalities associated with obesity and diabetes have the potential to significantly sustain cancer, we investigated whether the contribution of adipocytes into BC progression might be modulated by metabolic alterations (i.e. glucose levels). Thus, we started from an "hyperglycemic-like condition" to simulate a reduction of glucose levels. To this aim, BC cells and mammary adipocytes were co-cultured

Gene symbol	Description	mRNA transcripts	log2 FC	*p*-val	adjusted *p*-val
*C1R***	Complement C1r	NM_001733	1.81	3.17E-08	7.29E-06
CACNB4	Calcium voltage-gated channel auxiliary subunit beta 4	NM_001145798	1.64	5.33E-05	3.71E-03
*APOE***	Apolipoprotein E	NM_001302689 NM_001302690 NM_001302688 NM_001302691	1.44 1.44 1.40 1.39	1.47E-07 1.53E-07 1.96E-07 2.22E-07	3.00E-05 3.10E-05 3.82E-05 4.10E-05
RARRES3	Retinoic acid receptor responder 3	NM_004585	1.28	9.50E-05	5.65E-03
*SLC29A4***	Solute carrier family 29 member 4	NM_001040661 NM_153247 NM_001300847	1.07 1.07 1.07	1.63E-04 1.58E-04 1.03E-04	8.42E-03 8.23E-03 5.96E-03
*APBB1***	Amyloid beta precursor protein binding family B member 1	NM_001257320 NM_001164 NM_145689	0.97 0.97 0.94	1.92E-04 9.32E-06 1.43E-05	9.50E-03 8.14E-04 1.20E-03
*ADCY7***	Adenylate cyclase 7	NM_001286057	0.96	7.11E-08	1.53E-05
GSDMB	Gasdermin B	NM_001165958 NM_001165959 NM_001042471 NM_018530	0.87 0.87 0.86 0.85	9.99E-05 1.12E-04 1.21E-04 1.13E-04	5.87E-03 6.34E-03 6.68E-03 6.36E-03
RASA4	RAS p21 protein activator 4	NM_001079877 NM_006989	0.85 0.84	5.86E-05 9.30E-05	3.93E-03 5.61E-03
RASA4B	RAS p21 protein activator 4B	NM_001277335	0.85	5.18E-05	3.64E-03
FAM171A1	Family with sequence similarity 171 member A1	NM_001010924	0.79	4.89E-05	3.48E-03
LRP1	LDL receptor related protein 1	NM_002332	0.77	4.62E-05	3.32E-03
*CRLF1***	Cytokine receptor like factor 1	NM_004750	0.70	3.64E-05	2.70E-03
*CCDC74A***	Coiled-coil domain containing 74 A	NM_001258306 NM_138770	0.68 0.64	6.06E-05 6.11E-05	3.96E-03 3.97E-03
*PALM***	Paralemmin	NM_001040134 NM_002579	0.67 0.67	7.37E-06 6.80E-06	6.78E-04 6.39E-04
MFGE8	Milk fat globule-EGF factor 8 protein	NM_001310320 NM_005928 NM_001310321	0.67 0.65 0.61	3.49E-05 4.75E-05 1.53E-04	2.61E-03 3.40E-03 8.05E-03
*MXRA7***	Matrix remodeling associated 7	NM_001008528	0.66	1.31E-04	7.13E-03
*HSPB1***	Heat shock protein family B (small) member 1	NM_001540	0.63	9.38E-05	5.64E-03
HDAC11	Histone deacetylase 11	NM_001136041	0.61	1.79E-04	9.05E-03
*PCOLCE***	Procollagen C-endopeptidase enhancer	NM_002593	0.54	3.29E-05	2.50E-03
*SPHK1***	Sphingosine kinase 1	NM_182965 NM_001142601	0.53 0.49	3.79E-05 1.78E-04	2.79E-03 9.05E-03
MIDN	Midnolin	NM_177401	0.53	1.45E-05	1.22E-03
PPP1R26	Protein phosphatase 1 regulatory subunit 26	NM_014811	0.49	2.30E-05	1.83E-03
*TIMP2***	TIMP metallopeptidase inhibitor 2	NM_003255	0.45	6.78E-06	6.39E-04
*CMTM3***	CKLF like MARVEL transmembrane domain containing 3	NM_144601 NM_181553	0.45 0.45	1.40E-04 1.50E-04	7.57E-03 7.96E-03
*TWF2***	Twinfilin actin binding protein 2	NM_007284	0.41	2.76E-06	3.29E-04
*VAT1***	Vesicle amine transport 1	NM_006373	0.41	2.43E-06	2.95E-04
GDF11	Growth differentiation factor 11	NM_005811	0.38	3.61E-07	6.24E-05
DBN1	Drebrin 1	NM_004395	0.38	1.69E-05	1.39E-03
*SERPINH1***	Serpin family H member 1	NM_001207014 NM_001235	0.32 0.32	2.74E-06 2.89E-06	3.28E-04 3.40E-04
*INF2***	Inverted formin. FH2 and WH2 domain containing	NM_001031714 NM_022489	0.32 0.31	6.59E-06 8.07E-06	6.26E-04 7.25E-04
POLRMT	RNA polymerase mitochondrial	NM_005035	0.31	5.50E-06	5.47E-04
KLHL42	Kelch like family member 42	NM_020782	-0.31	1.50E-04	7.96E-03
SLC25A4	Solute carrier family 25 member 4	NM_001151	-0.33	5.69E-05	3.90E-03
BLZF1	Basic leucine zipper nuclear factor 1	NM_001320973	-0.34	1.69E-05	1.39E-03
MYO1B	Myosin IB	NM_001330238 NM_001130158 NM_001161819 NM_001330237	-0.47 -0.47 -0.47 -0.47	1.96E-04 1.87E-04 1.91E-04 1.81E-04	9.67E-03 9.34E-03 9.48E-03 9.14E-03
*CITED2**	Cbp/p300 interacting transactivator with Glu/Asp rich carboxy-terminal domain 2	NM_006079 NM_001168389 NM_001168388	-0.48 -0.50 -0.50	3.57E-05 5.90E-06 5.33E-06	2.65E-03 5.72E-04 5.32E-04
*PLK2**	Polo like kinase 2	NM_006622 NM_001252226	-0.55 -0.55	1.90E-05 1.52E-05	1.55E-03 1.27E-03

Continued

Gene symbol	Description	mRNA transcripts	log2 FC	*p*-val	adjusted *p*-val
*TUFT1**	Tuftelin 1	NM_001126337 NM_020127 NM_001301317	-0.56 -0.56 -0.56	2.67E-05 2.78E-05 2.69E-05	2.11E-03 2.17E-03 2.12E-03
*ARSD**	Arylsulfatase D	NM_001669	-0.57	1.41E-04	7.57E-03
*BCAR3**	Breast cancer anti-estrogen resistance 3	NM_003567 NM_001261408 NM_001261409 NM_001261410	-0.80 -0.81 -0.81 -0.84	1.48E-06 9.75E-07 1.01E-06 1.30E-07	1.94E-04 1.42E-04 1.47E-04 2.71E-05
*ANTXR2**	Anthrax toxin receptor 2	NM_001286781 NM_058172 NM_001286780	-0.81 -0.82 -0.85	1.45E-04 1.10E-04 1.65E-04	7.71E-03 6.22E-03 8.49E-03
CTGF	Connective tissue growth factor	NM_001901	-1.45	2.27E-05	1.81E-03
*NEDD9**	Neural precursor cell expressed. developmentally down-regulated 9	NM_182966	-2.64	3.44E-05	2.59E-03

Table 2. DETs in co-cultured MCF7 $_{HG}$*vs* MCF7 $_{HG}$ * UP-regulated in Co-cultured MCF7 $_{HG-> LG}$*vs* Co-cultured MCF7 $_{HG}$; ** DW-regulated in Co-cultured MCF7 $_{HG-> LG}$*vs* Co-cultured MCF7 $_{HG}$.

while exposed to basal 25mM glucose (High Glucose, HG) or shifted to 5.5mM glucose (Low Glucose; LG), resembling hyperglycemia or normoglycemia in humans, respectively. By RNA-Seq we described the reciprocal reprogramming of co-cultured cells. At first, we observed that MCF7 BC cell transcriptome is highly modified in presence of adipocytes independently of glucose levels. The most striking feature we noticed is that "adipogenesis-related" genes were differentially regulated in BC cells upon co-culture with adipocytes; notably, the activation of the adipogenic program (i.e. up-regulation of *PPARG*, *INSR*, *CEBPD*) predominantly occurs in ER^+, PR^+, HER^- BC cells, in HG. On the other hand, a de-differentiation program is induced in adipocytes, when co-cultured with BC cells in LG. Such effect is suggested by the decrease of adipogenic genes (i.e. *PPARG*, *CEBPA*) and further confirmed by Oil Red O staining and confocal microscopy analysis. Interestingly, we also found the induction of pluripotency markers (i.e. *OCT4*, *SOX2* and *NANOG*) in adipocytes co-cultured with BC cells in LG. These observations led us to hypothesize that BC cells in presence of adipocytes may activate transcriptional patterns for their own lipid synthesis and accumulation, particularly in a glucose-rich environment; on the other hand, BC cells may induce adipocytes de-differentiation and enhanced lipids release predominantly upon glucose lowering as source of nutrients. However, whether BC cells also enhance their fatty acid uptake needs to be further determined.

Adipogenic and pluripotency genes were also measured in BC cell lines with different receptor patterns when co-cultured with adipocytes under different glucose concentration. Overall, only slight glucose-induced modifications were found, indicating a cell type-specific effect. Similarly, co-culture with various BC cell types induced no change in adipogenic and pluripotency genes as well as in lipid content in adipocytes. Of note, a different crosstalk between BC subtypes and the tumor microenvironment is well documented in literature[24]. Therefore, such aspect needs to be further investigated, both in other BC cell lines and in human samples.

Adipocytes represent a preferential source of lipids for cancer cells. Consistently, both *in vivo* and *in vitro* experiments have demonstrated that adipocytes in BC exhibit extensive phenotypical changes leading to de-lipidation, decreased size, occurrence of activated phenotype and morphological changes toward a fibroblast-like shape, leading to enrichment of adipocyte-derived fibroblasts (ADFs)[8,18,19].

Importantly, adipocytes may act as a therapeutic obstacle, as they are involved in mechanisms of resistance against various therapies for BC[19,22]. Normal adipocyte size heterogeneity is lost in obesity and several epidemiological studies reported that large amounts of adipose tissues are closely associated with poor prognosis for BC, independently of menopause status, tumor stage, and hormone status[13,25]. In addition, weight gain in BC survivors is associated with adverse health consequences[5,16]. Hyperinsulinemia and T2D are also independent risk factors for poor prognosis in women with BC[4,16]. Although metabolic changes may not cause malignancy, they most likely contribute to tumor progression. Indeed, cancer cells need to proliferate rapidly and to maintain a constant supply of lipids and lipid precursors to fuel membrane production[8,9]. Thus, improving knowledge of adipocytes/CAAs functions might help to decipher the relationship between obesity and/or diabetes and the poor clinical outcome in BC. Our group reported that adipocytes are able to integrate inputs from the metabolic environment (i.e. glucose and free fatty acids) and secrete a higher amount of IGF-1 (Insulin Growth Factor 1), CCL-5 (C-C motif chemokine Ligand 5) and IL-8 (Interleukin 8). In turn, IGF-1 and CCL-5, respectively, promote growth and invasiveness of BC cells[20,21] and IL-8 reduces BC cell drug responsiveness[22].

Here, we described impact of glucose onto transcriptomic changes reciprocally induced by cancer and adipose cells. We provide evidence that co-culture with adipocytes in a glucose rich environment determined a re-program of BC cell transcriptome driving lipid accumulation, an hallmark of BC aggressiveness[26,27]. In agreement with histological evidence indicating that the periphery of BC has a low fibroblast/adipocyte ratio, whereas this ratio is higher toward the center[28], our data point out to a transcriptional effect through which BC cells induce adipocytes de-lipidation, paralleled by pluripotency gain, a as source of lipids when glucose lowering occurs.

As the tumor microenvironment actively participates in tumor progression and metastasis rather than acting as a by-stander, therapeutic strategies targeting the tumor microenvironment hold great potential. Here, we demonstrated that adipocytes in HG sustain the acquisition of stem-like properties in BC cells, also reducing

Gene symbol	Description	mRNA transcripts	log2 FC	*p*-val	adjusted *p*-val
CNR1	Cannabinoid receptor 1	NM_001160259 NM_001160258 NM_016083 NM_001160226	2.22 2.20 2.20 2.20	2.09E-07 3.48E-07 3.15E-07 3.15E-07	4.53E-05 6.39E-05 5.89E-05 5.89E-05
RASD1	Ras related dexamethasone induced 1	NM_001199989 NM_016084	1.87 1.85	9.97E-05 1.18E-04	6.51E-03 7.33E-03
ANK2	Ankyrin 2	NM_001148	1.37	8.93E-05	5.99E-03
TIMP3	TIMP metallopeptidase inhibitor 3	NM_000362	0.82	2.79E-05	2.29E-03
CBLB[*]	Cbl proto-oncogene B	NM_001321797 NM_001321820 NM_001321791 NM_001321808 NM_001321799 NM_001321796 NM_001321790 NM_001321798 NM_001321794 NM_001321793 NM_001321788 NM_001321813 NM_001321816 NM_001321806 NM_001321795 NM_170662 NM_001321807 NM_001321789 NM_001321822 NM_001321786 NM_001321811	0.58 0.58 0.58 0.58 0.58 0.58 0.58 0.57 0.57 0.57 0.57 0.56 0.56 0.56 0.56 0.55 0.55 0.55 0.55 0.55 0.55	6.97E-06 1.31E-05 1.25E-05 1.31E-05 7.59E-06 1.09E-05 1.45E-05 1.11E-05 1.58E-05 1.97E-05 2.63E-05 2.06E-05 2.22E-05 5.14E-05 2.40E-05 3.97E-05 4.14E-05 3.69E-05 4.34E-05 5.73E-05 4.77E-05	7.85E-04 1.26E-03 1.22E-03 1.26E-03 8.28E-04 1.10E-03 1.35E-03 1.10E-03 1.44E-03 1.73E-03 2.17E-03 1.77E-03 1.89E-03 3.81E-03 2.01E-03 3.09E-03 3.19E-03 2.92E-03 3.33E-03 4.14E-03 3.60E-03
FAM216A	Family with sequence similarity 216 member A	NM_013300	0.50	1.04E-04	6.68E-03
LPIN2[*]	Lipin 2	NM_014646	0.44	3.80E-05	2.98E-03
WWC2[*]	WW and C2 domain containing 2	NM_024949	0.38	4.04E-05	3.12E-03
SNAPC1	Small nuclear RNA activating complex polypeptide 1	NM_003082	0.37	1.03E-04	6.65E-03
SKIL	SKI like proto-oncogene	NM_005414 NM_001145098 NM_001248008 NM_001145097	0.31 0.31 0.31 0.31	1.08E-04 1.71E-04 1.14E-04 1.48E-04	6.88E-03 9.73E-03 7.20E-03 8.70E-03
XPOT[*]	Exportin for tRNA	NM_007235	0.23	1.75E-04	9.85E-03
APEX1	Apurinic/apyrimidinic endodeoxyribonuclease 1	NM_080649 NM_080648	0.23 0.23	1.32E-04 1.69E-04	7.93E-03 9.62E-03
DDX50[*]	DExD-box helicase 50	NM_024045	0.21	1.07E-05	1.08E-03
FBX09	F-box protein 9	NM_033480	-0.22	8.21E-05	5.56E-03
MAPK3[**]	Mitogen-activated protein kinase 3	NM_001109891 NM_002746	-0.30 -0.32	1.24E-04 4.03E-05	7.62E-03 3.12E-03
ZFYVE[**]	Zinc finger FYVE-type containing 19	NM_001077268 NM_001258420 NM_001258421 NM_032850	-0.36 -0.36 -0.38 -0.39	2.04E-05 2.31E-05 2.37E-05 1.55E-05	1.77E-03 1.96E-03 1.99E-03 1.43E-03
LMNA[**]	Lamin A/C	NM_001257374 NM_170708 NM_170707 NM_001282624 NM_001282626 NM_001282625 NM_005572	-0.42 -0.42 -0.43 -0.43 -0.43 -0.43 -0.43	1.79E-05 2.21E-06 2.09E-06 7.15E-06 1.80E-06 5.03E-06 5.12E-06	1.59E-03 3.14E-04 2.99E-04 7.91E-04 2.70E-04 6.08E-04 6.16E-04
EPB41L[**]	Erythrocyte membrane protein band 4.1 like 2	NM_001431	-0.76	3.16E-05	2.54E-03
ADGRB[**]	Adhesion G protein-coupled receptor B2	NM_001294335 NM_001294336	-1.02 -1.02	2.03E-06 2.34E-06	2.93E-04 3.24E-04
NXPH3[**]	Neurexophilin 3	NM_007225	-1.17	9.83E-05	6.45E-03
ARRDC4[**]	Arrestin domain containing 4	NM_183376	-1.34	1.84E-05	1.63E-03
ARL4D[**]	ADP ribosylation factor like GTPase 4D	NM_001661	-1.50	5.75E-05	4.14E-03
TXNIP[**]	Thioredoxin interacting protein	NM_006472 NM_001313972	-2.20 -2.22	4.03E-10 3.54E-10	1.77E-07 1.61E-07

Table 3. DETs in co-cultured MCF7 $_{HG-> LG}$*vs* MCF7 $_{HG-> LG}$ UP-regulated in Co-cultured MCF7 $_{HG-> LG}$vs. Co-cultured MCF7 $_{HG}$; ** DW-regulated in Co-cultured MCF7 $_{HG-> LG}$vs. Co-cultured MCF7 $_{HG}$.

their responsiveness to Tamoxifen treatment. Modulating the plasticity of adipocytes and elucidating their extracellular and intracellular signaling pathways are major challenges for future research in this field. Indeed, molecules linked to adipocyte biology might offer new prognostic tools and therapeutic opportunities for treating cancer in diabetic/obese patients.

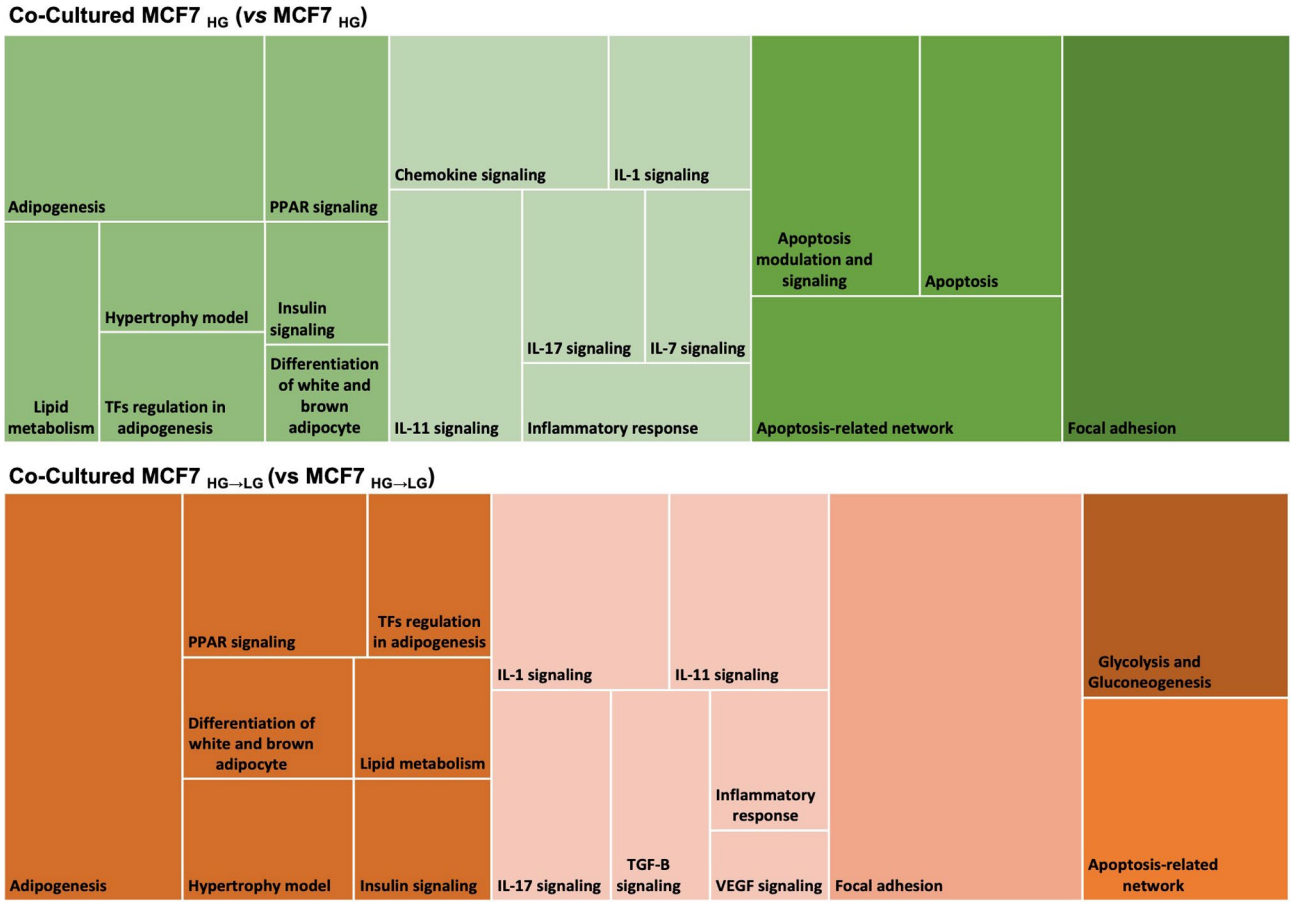

Figure 4. Pathway analysis of DEGs in BC cells. Selected processes (Z-score > 1.5) from pathway enrichment of DEGs (p-val < 0.05) in Co-Cultured MCF7 $_{HG}$ (*vs* MCF7 $_{HG}$) and Co-Cultured MCF7 $_{HG-> LG}$ (*vs* MCF7 $_{HG-> LG}$). Color grading groups related processes. The size of each square reflects the number of DEGs involved in the process.

Overall, our results provide additional cues to define the role of glucose in the dialogue between adipose and cancer cells in breast and, therefore, for BC managements in the concurrence of obesity/diabetes.

Methods

Cell cultures

MCF7 (ER$^+$, PR$^+$, HER2$^-$), BT474 (ER$^+$ HER$^+$ PR$^-$), SKBR3 (ER$^-$ HER$^+$ PR$^-$) and MDA-MB231 (ER$^-$ HER$^-$ PR$^-$) human BC cells, available in our laboratory, were cultured in Dulbecco's modified Eagle's medium (DMEM), supplemented with 10% fetal bovine serum (FBS), 2 mM glutamine, 100 units/ml penicillin and 100 units/ml streptomycin. Cultures were maintained in a humidified atmosphere of 95% air and 5% CO2 at 37 °C.

Human adipose tissue samples were obtained from mammary adipose biopsies of healthy woman undergoing surgical mammary reduction, free of neoplastic, metabolic or endocrine diseases. Informed consent was obtained before the surgical procedure ap-proved by the ethical committee of the University of Naples "Federico II". Mammary Adipose derived Mesenchymal Stem Cells (MAd-MSCs) were isolated from the Stromal Vascular Fraction, as described in Ambrosio et al. (2017)[22], and cultured in DMEM, supplemented with 10% fetal bovine serum (FBS), 2 mM glutamine, 100 units/ml penicillin and 100 units/ml streptomycin in 25mM glucose. Media, sera and antibiotics for cell culture were from Lonza (Basel, Switzerland).

Adipocyte differentiation

Adipocyte differentiation of MAd-MSCs was obtained by the alternation (every three days, two times) of an Adipocyte differentiation Induction Mix (AIM) - containing 850 nM Insulin, 10 µM Dexamethasone, 0.5 mM 3-IsoButyl-1-MethylXanthine, 33 µM Biotin, 17 µM Pantothenate and 1 µM Rosiglitazone - and an Adipocyte differentiation Maintaining Mix (AMM) consisting of 850 nM Insulin and 1 µM Rosiglitazone. Then, the cells were stimulated (every two days, two times) with 1 µM Rosiglitazone. Adipocyte differentiation of MAd-MSCs was reached in 15–17 days. Lipid accumulation was determined by Oil red O staining[14,29] and assessed by optical density determination at 510 nm using a microplate reader. All the chemicals for adipocyte differentiation were from Sigma-Aldrich (St Louis, MO, USA).

High-content imaging and analysis

For fluorescence-based lipid quantification we used the OPERA Phenix Plus High Content Imaging system (Revvity). Images were acquired with a 10x air objective. A first laser with a wavelength of 375 nm was utilized to identify the cell nuclei stained with Hoechst 33,342 (Invitrogen, MA, USA), while a second laser with a wavelength of 488 nm was used to identify lipid droplets using Bodipy-488. For image analysis, we used the Harmony High-Content Imaging and Analysis Software, which provides an easy quantification of complex cellular phenotypes. First, individual cell nuclei were identified using the Hoechst 33,342 channel. Next, the cell regions were identified by "Ring region" resize option. Finally, lipid droplets were captured by "Find spots" function using the Bodipy-488 channel.

Establishment of 2D co-cultures

Adipocyte differentiation of MAd-MSCs was carried out in the bottom chamber of a transwell culture system (0.4 µm pore size, Costar, Cambridge, MA, USA). At the 15th days of the process, fully differentiated adipocytes were obtained. Thus, BC cells were seeded in the upper chamber of the system upon a washout step to remove potential confounding effects from Rosiglitazone. Adipocytes and BC cells were co-cultured for 4 days while exposed to basal 25mM glucose (High Glucose; HG) or shifted to 5.5mM glucose (Low Glucose; LG). In parallel, both BC cells and adipocytes were mono-cultured in HG or shifted to LG. Adipocytes and BC cells, from three independent experiments, were processed to obtain RNA samples for RNA sequencing (Adipocytes, MCF7) or qPCR (Adipocytes, MCF7, BT474, SKBR3 and MDA-MB231). Cell lysates from MCF7 and adipocytes were obtained for Western Blot analysis. Co-Cultured MCF7 were treated with Tamoxifen (5µM) while exposed to HG or shifted to LG. Conditioned media were collected from co-cultures of MCF7 and adipocytes (HG or shifted in LG) and used to set up Mammosphere-forming assay (see below).

Mammosphere-forming assay

MCF7 cells from co-cultures exposed to HG or shifted to LG were plated in ultra-low attachment 96-wells with or without respective conditioned media (HG or LG); as a control, monocultured MCF7 were plated in HG or LG medium. After 10 days, mammosphere number was quantified (number of formed spheres/number of wells containing cells × 100)[14]. In parallel, mammosphere diameter was measured by a software associated to the Olympus DP20 microscope digital camera system.

Cell survival assay

Cell viability in 2D system was analyzed by using sulforhodamine B[30]. Spheroid viability was determined by CellTiter-Glo 3D Cell Viability Assay (Promega, Madison, Wisconsin, USA), according to the manufacturer's instructions.

RNA isolation and analysis

Total RNA was isolated from cells using TRIzol solution (Life Technologies, Carlsbad, CA, USA) according to the manufacturer's instructions. All RNA samples were quantified by measuring the absorbance at 260 nm and 280 nm (NanoDrop spectrophotometer, Life Technologies, CA, USA). The integrity of RNA samples was further analyzed by using the digital electrophoresis system Experion with the "RNA StdSens Kit" (Biorad, CA, USA), following the manufacturer's instructions. The run and result analysis were per-formed by the Experion software. RNA samples with a RNA Quality Indicator (RQI) value ≥ 9 were considered good for the further analysis.

RNA-sequencing

Paired-end cDNA libraries were prepared for sequencing on the Illumina Hi-Seq 2500 platform, available at IGA Technology Service (Udine, Italy). Paired-end RNA-sequencing reads were aligned against the human genome assembly GRCh37 using STAR version 2.4.2a using default settings[31]. All samples passed quality checks at default settings. All raw and processed RNA-Seq data files have been deposited at the NCBI Gene Expression Omnibus repository with GEO accession number GSE243555. To quantify transcriptome features we used Ensembl genome annotation version 90 and for gene level quantification we used HTseq version 0.11.1[32]. Gene-level differential analysis was carried out at transcript-level resolution by using R package DeSeq2[33]. A p-val < 0.05 was used to select differentially expressed transcripts (DETs). Pathway analysis was performed using PathVisio.

RT-PCR

RNA samples were reverse-transcribed using SuperScript III Reverse Transcriptase with oligo dT primers (Life Technologies, CA, USA) according to the manufacturer's instructions. To check the amplifiable template RNA/cDNA, RT-PCR amplification of housekeeping genes was performed. Amplification reactions were set up using AmpliTaq Gold (Life Technologies, CA, USA) and specific primer pairs, designed by Oligo 4.0 (Supplementary Table S5).

Quantitative real-time PCR (qPCR)

qPCR was performed using an iTaq Universal SYBR Green Supermix (Biorad, CA, USA), according to the manufacturer's instructions for the CFX Connect Real-Time system (Biorad, CA, USA). Relative quantification of gene expression was measured by using $2 - \Delta\Delta Ct$ method. Expression levels were normalized for the reference sample using peptidylprolyl isomerase A (PPIA) as housekeeping gene.

Western blot

Whole-cell lysates were obtained using RIPA lysis buffer supplemented with Halt Protease and Phosphatase Inhibitor Cocktail (Thermo Fisher Scientific, Waltham, Massachusetts, USA) and quantified by Bradford Assay

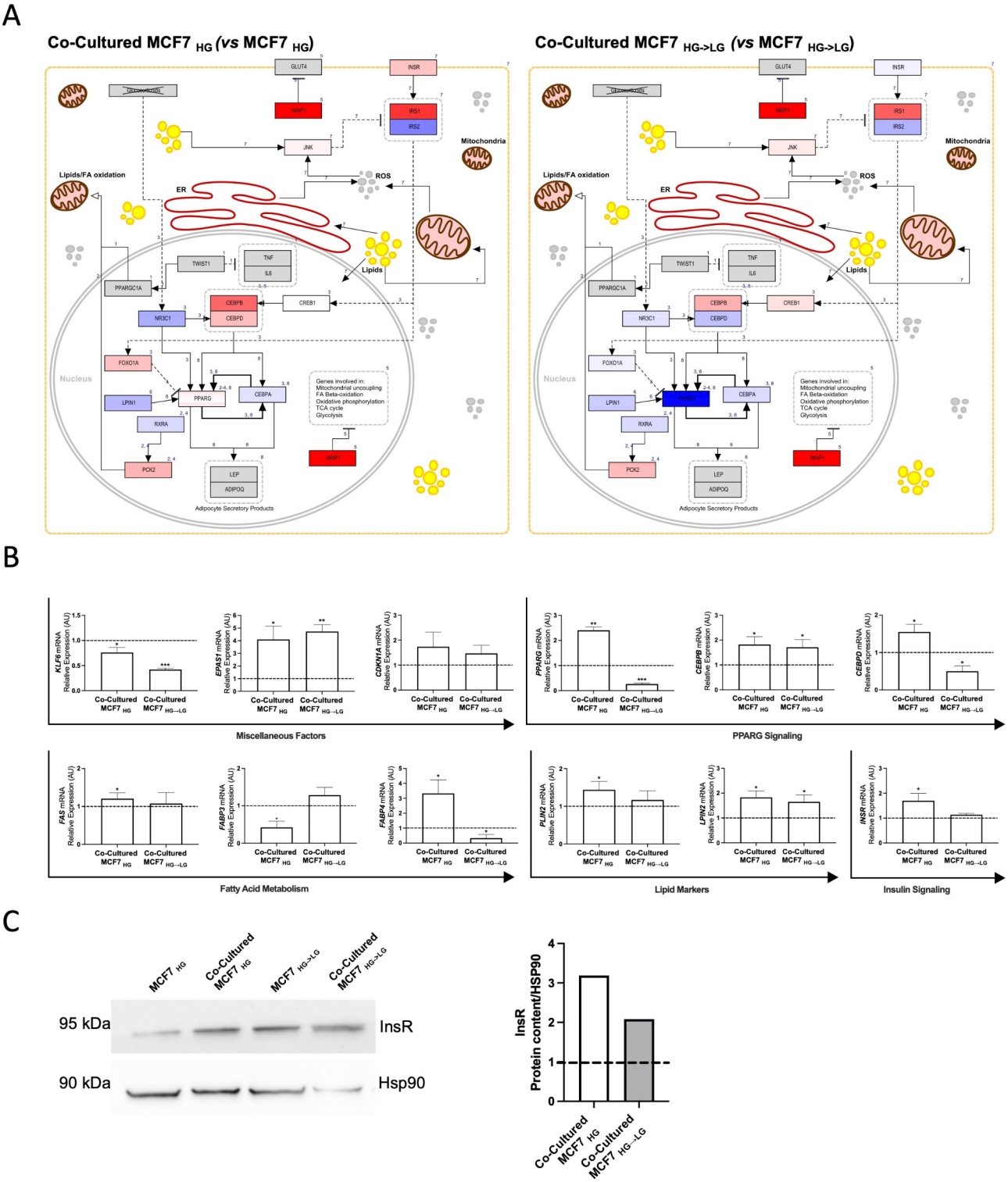

Reagent (Bio-Rad, Hercules, CA, USA). For each sample, 40–60 mg of proteins were used for western blot analysis. According to manufacturer's instructions, primary antibodies were used to different dilutions: anti-PPARγ (1:1000, Cell Signaling Technology, Danvers, Massachusetts, USA), and anti-IR (1:500, Cell Signaling Technology, Danvers, Massachusetts, USA). Anti-Hsp90 (1:5000; Origene, Rockville, Maryland, USA) was used as a loading control antibody. Secondary anti-IgG (mouse and rabbit) antibodies were used at dilution 1:5000 (Bio-Rad, Hercules, CA, USA). Pierce ECL Western Blotting Substrate (Thermo Fisher Scientific, Waltham, Massachusetts, USA) was used for detection of immunoreactive bands by ChemiDoc Imaging System (BioRad). Quantification of protein levels (pixel density) was performed by GelQuant.NET software (www.biochemlabsolutions.com). Intensity values were normalized on Hsp90 expression and reference sample.

Figure 5. Glucose-modulated adipogenic markers in MCF7 BC cells co-cultured with adipocytes. MCF7 were co-cultured with adipocytes (4 days) while exposed to basal 25mM (Co-Cultured MCF7 $_{HG}$) or shifted to 5.5mM (Co-Cultured MCF7 $_{HG->LG}$) glucose. A) Representative images of adipogenic process in Co-Cultured MCF7 $_{HG}$ (*vs* mono-cultured MCF7 $_{HG}$) and Co-Cultured MCF7 $_{HG->LG}$ (*vs* monocultured MCF7 $_{HG->LG}$). Red color indicates UP-regulated genes; blue color indicates DW-regulated genes (p-val<0.05). B) mRNA expression levels of adipogenesis-related markers. Data were normalized on the Ribosomal Protein S2 (*RPS23*) gene as internal standard. Results were represented as bar graph of 3–5 independent triplicate experiments showing mRNA levels in Co-Cultured MCF7 $_{HG}$ and Co-Cultured MCF7 $_{HG->LG}$ as relative expression ($2^{-\Delta\Delta Ct}$) compared to that in monocultured MCF7 $_{HG}$ and MCF7 $_{HG->LG}$, respectively (control cells, dotted line). * denotes statistically significant values compared with monocultured cells (*p-val < 0.05; ** p-val < 0.01). C) Representative Western blot showing InsR protein levels in Co-Cultured or mono-cultured MCF7 $_{HG/HG->LG.}$ Hsp90 was used as loading control. Pixel density analysis was carried out to obtain InsR/Hsp90 ratio for each sample. Bar graphs show the relative amount of InsR protein levels (Fold over basal; dotted line) in Co-Cultured MCF7 $_{HG}$ and Co-Cultured MCF7 $_{HG->LG}$ compared to that in monocultured MCF7$_{HG}$ and MCF7 $_{HG->LG}$, respectively. See Supplementary FigureS1-A.

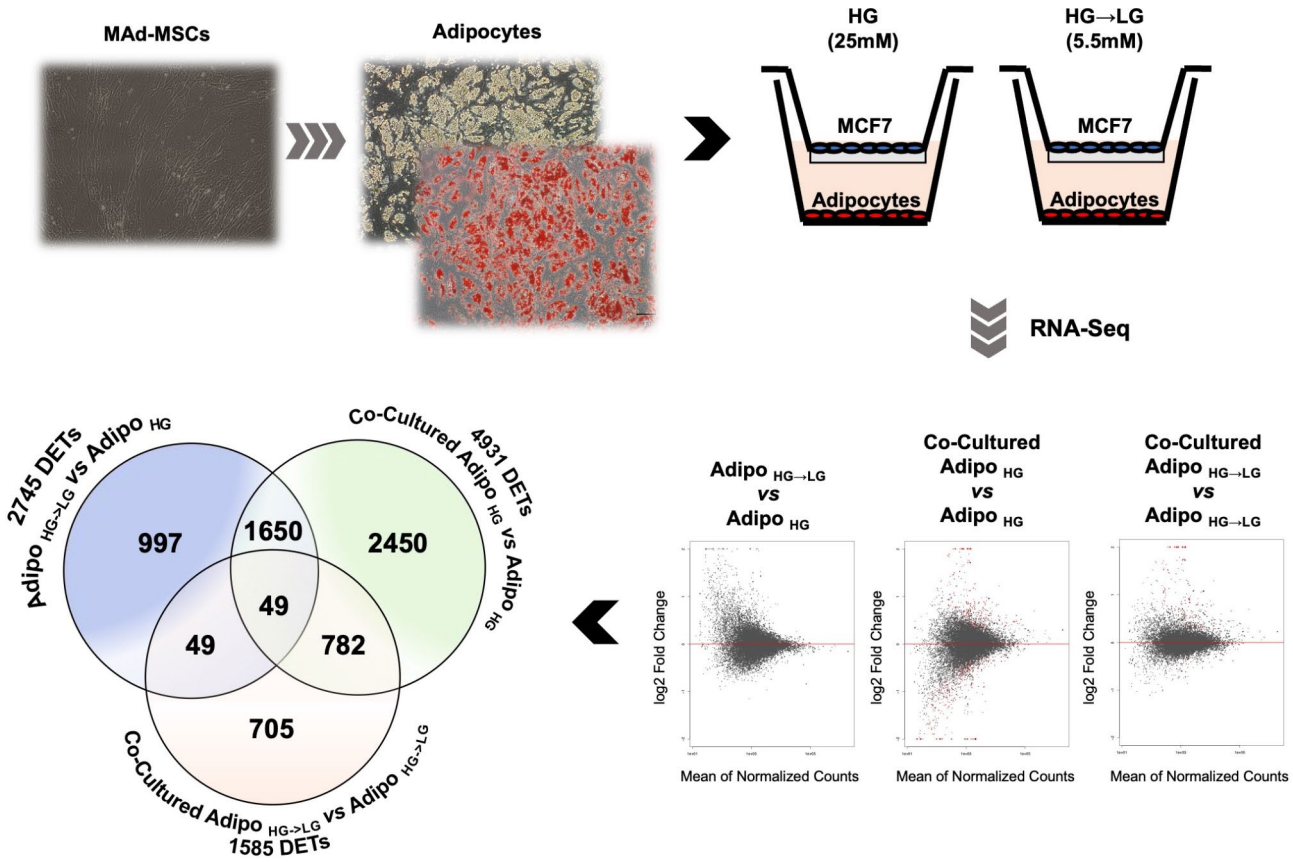

Figure 6. Effect of glucose and/or MCF7 BC cell on adipocytes transcriptome. Schematic representation of the experiment: Adipose-derived Mesenchymal Stem Cells (MAd-MSCs) were differentiated into mature adipocytes on the bottom chamber of a transwell system. At the 15th days of the differentiation process, MCF7 were seeded in the upper chamber of the system. Adipocytes were co-cultured with BC cells for 4 days while exposed to basal 25mM glucose (High Glucose, HG; Co-Cultured Adipo $_{HG}$) or shifted to 5.5mM glucose (Low Glucose, LG; Co-Cultured Adipo $_{HG-> LG}$). In parallel, adipocytes were mono-cultured in basal HG (Adipo $_{HG}$) or shifted to LG (Adipo $_{HG-> LG}$). RNA samples from three independent experiments were obtained for RNA-Seq. Computational data analysis provided Differentially Expressed Transcripts (DETs; p-val < 0.05) from Adipo $_{HG-> LG}$*vs* Adipo $_{HG}$ (Glucose lowering), Co-Cultured Adipo $_{HG}$*vs* Adipo $_{HG}$ (Co-culture with BC cells in HG) and Co-Cultured Adipo $_{HG-> LG}$*vs* Adipo $_{HG-> LG}$ (Co-culture with BC cells in LG) comparisons. Unique or common DETs were discriminated by intersecting lists of DETs.

Gene symbol	Description	mRNA transcripts	log2 FC	*p*-val
ZNF784	Zinc finger protein 784	NM_203374	0.66	1.2E-02
PAG1	Phosphoprotein membrane anchor with glycosphingolipid microdomains 1	NM_004430	0.60	1.49E-02
RASSF7	Ras association domain family member 7	NM_001143993 NM_003475	0.60 0.56	9.75E-03 2.29E-02
HK2	Hexokinase 2	NM_000189	0.53	1.92E-02
PLIN2	Perilipin 2	NM_001122	0.51	4.50E-02
ABCB9	ATP binding cassette subfamily B member 9	NM_001243014	0.45	2.62E-02
RAD51B	RAD51 paralog B	NM_001321815	0.43	1.60E-02
ABCB9	ATP binding cassette subfamily B member 9	NM_203444	0.43	3.53E-02
RFC3	Replication factor C subunit 3	NM_181558	0.42	2.95E-02
ENTPD5	Ectonucleoside triphosphate diphosphohydrolase 5	NM_001321984	0.40	3.53E-05
RAD51B	RAD51 paralog B	NM_001321817 NM_001321810 NM_133510 NM_001321818 NM_001321814	0.40 0.40 0.38 0.38 0.36	3.10E-02 2.74E-02 4.17E-02 3.54E-02 4.12E-02
ENTPD5	Ectonucleoside triphosphate diphosphohydrolase 5	NM_001321987 NM_001321985 NM_001249 NM_001321986 NM_001321988	0.21 0.21 0.21 0.20 0.19	7.13E-03 7.13E-03 7.13E-03 9.50E-03 1.22E-02
PASK	PAS domain containing serine/threonine kinase	NM_015148 NM_001252119 NM_001252122	-0.47 -0.47 -0.48	2.64E-02 2.65E-02 2.44E-02
SLC19A1 *PASK*	Solute carrier family 19 member 1 PAS domain containing serine/threonine kinase	NM_001205207 NM_001252120	-0.48 -0.49	2.62E-02 2.17E-02
FIBCD1	fFbrinogen C domain containing 1	NM_001145106 NM_032843	-0.56 -0.56	3.90E-02 3.70E-02
OMD	Osteomodulin	NM_005014	-0.69	3.13E-02
WDR97	WD repeat domain 97	NM_001316309	-0.70	3.56E-02
ARRDC4	Arrestin domain containing 4	NM_183376	-0.85	5.31E-03
TNFRSF6B	TNF receptor superfamily member 6b	NM_003823	-0.87	3.30E-03
TPGS1	Tubulin polyglutamylase complex subunit 1	NM_033513	-0.91	3.02E-02
TXNIP	Thioredoxin interacting protein	NM_001313972 NM_006472	-1.29 -1.29	2.51E-04 2.21E-04

Table 4. DETs in co-cultured Adipo $_{HG-> LG}$ vs. co-cultured Adipo $_{HG}$

Statistical analysis

Statistical analyses were performed using GraphPad Prism 7.0 software (GraphPad Software Inc., CA, USA). One sample t test was applied for pairwise comparisons; p-val < 0.05 was considered statistically significant.

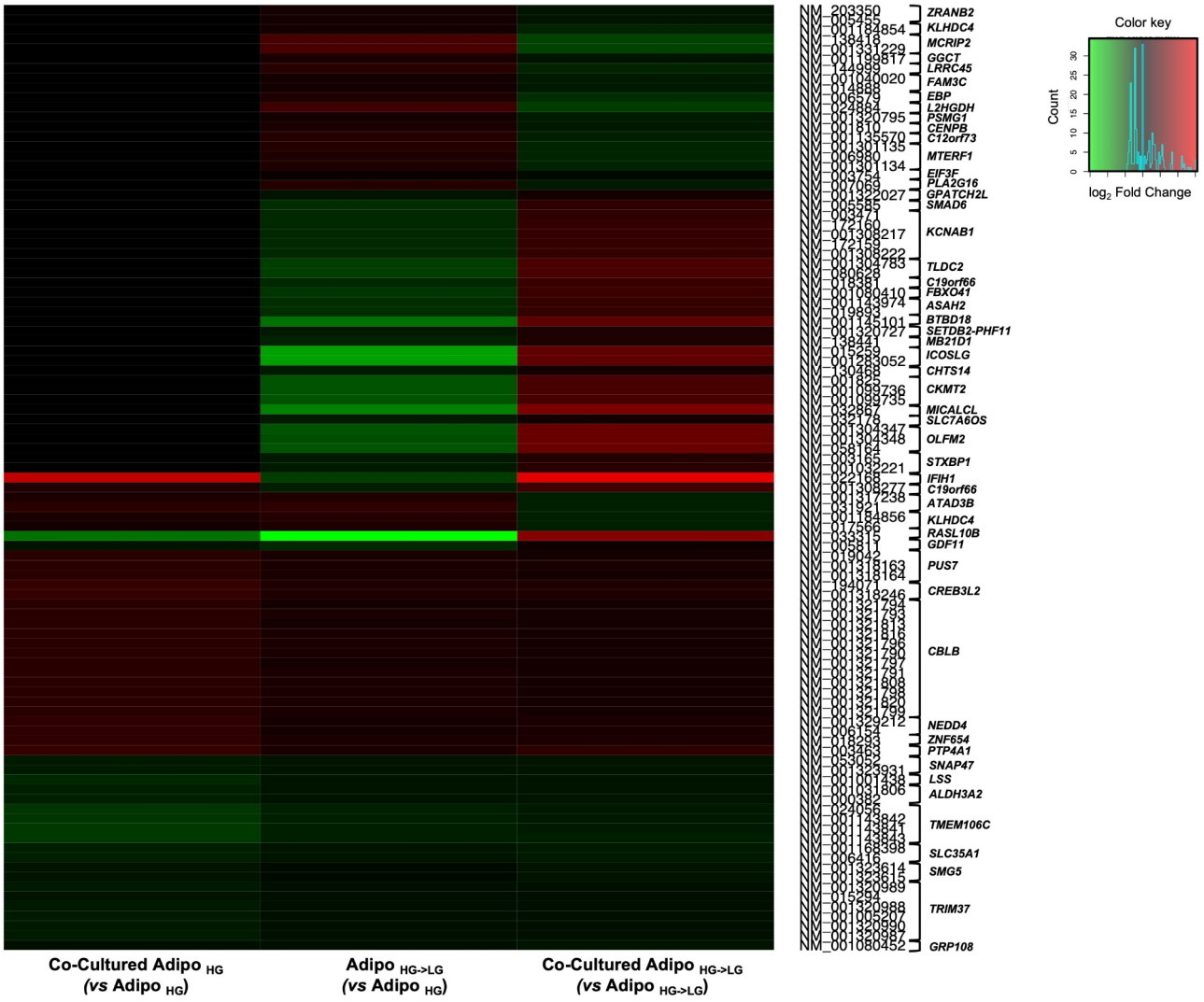

Figure 7. Commonly modulated genes by glucose and MCF7 BC cells in adipocytes. Normalized expression values of transcripts commonly modulated in adipocytes by BC cells (Co-Cultured Adipo $_{HG}$*vs* Adipo $_{HG}$), glucose lowering (Adipo $_{HG-> LG}$*vs* Adipo $_{HG}$) and glucose lowering + BC cells (Co-Cultured Adipo $_{HG-> LG}$*vs* Adipo $_{HG-> LG}$).

Gene symbol	Description	mRNA transcripts	log2 FC	*p*-val	adjusted *p*-val
EGR3	Early growth response 3	NM_004430 NM_001199881 NM_001199880	1.53 1.52 1.52	6.87E-04 7.05E-04 6.87E-04	4.30E-02 4.33E-02 4.30E-02
PDK3	Pyruvate dehydrogenase kinase 3	NM_005391	1.42	3.60E-04	3.04E-02
PRKD2	Protein kinase D2	NM_001079881	0.42	6.87E-04	4.30E-02
RBPJ	Recombination signal binding protein for immunoglobulin kappa J region	NM_203284	0.35	4.05E-04	3.06E-02
PTER	Phosphotriesterase related	NM_001261838	0.35	3.83E-04	3.06E-02
CHD6	Chromodomain helicase DNA binding protein 6	NM_032221	0.31	4.17E-04	3.10E-02
SMCHD1	Structural maintenance of chromosomes flexible hinge domain containing 1	NM_015295	0.24	5.96E-04	3.98E-02
LDOC1L	Leucine zipper down-regulated in cancer 1 like	NM_032287	0.22	4.43E-04	3.14E-02
ZNF148	Zinc finger protein 148	NM_021964	0.14	5.70E-04	3.84E-02
SIGMAR1	Sigma non-opioid intracellular receptor 1	NM_001282208 NM_005866 NM_001282207 NM_001282206 NM_001282205 NM_147157 NM_001282209	-0.35 -0.35 -0.35 -0.35 -0.34 -0.35 -0.35	9.52E-06 9.88E-06 1.17E-05 1.18E-05 1.89E-05 2.20E-05 2.58E-05	2.51E-03 2.58E-03 2.97E-03 2.98E-03 4.26E-03 4.65E-03 5.14E-03
SEC11C	Section 11 homolog C. signal peptidase complex subunit	NM_001010924	-0.56	4.65E-05	8.00E-03

Table 5. DETs in co-cultured Adipo $_{HG}$*vs* Adipo $_{HG}$

Gene symbol	Description	mRNA transcripts	log2 FC	*p*-val
HILPDA	Hypoxia inducible lipid droplet associated	NM_001098786 NM_013332	1.52 1.50	5.57E-03 5.59E-03
PRR5L	Proline rich 5 like	NM_001160169 NM_001160167 NM_024841 NM_001160168	0.88 0.87 0.86 0.85	4.14E-04 8.83E-04 1.65E-03 2.39E-03
*PLIN2**	Perilipin 2	NM_001122	0.87	6.32E-04
GYS1	Glycogen synthase 1	NM_002103 NM_001161587	0.83 0.83	1.61E-03 2.04E-03
SLC5A10	Solute carrier family 5 member 10	NM_001270649 NM_001042450 NM_152351	0.82 0.82 0.82	3.56E-03 3.62E-03 3.69E-03
TBX3	T-box 3	NM_013300	0.82	9.99E-03
IFI35	Interferon induced protein 35	NM_005533 NM_001330230	0.76 0.76	9.47E-03 9.48E-03
FAM162A	Family with sequence similarity 162 member A	NM_014367	0.67	5.63E-03
ERO1A	Endoplasmic reticulum oxidoreductase 1 alpha	NM_014584	0.66	2.30E-03
LPXN	Leupaxin	NM_001143995 NM_001307951 NM_004811	0.65 0.65 0.65	5.54E-03 5.76E-03 4.18E-03
DOHH	Deoxyhypusine hydroxylase/monooxygenase	NM_001145165 NM_031304	-0.52 -0.54	7.17E-03 6.21E-03
AQP11	Aquaporin 11	NM_173039	-0.55	3.22E-03
*SLC19A1***	Solute carrier family 19 member 1	NM_001205207	-0.58	7.87E-03
PLEKHG4	Pleckstrin homology and RhoGEF domain containing G4	NM_001129727 NM_001129731 NM_001129728 NM_001129729	-0.59 -0.60 -0.60 -0.60	4.69E-04 3.04E-04 3.35E-04 2.90E-04
*GLI4***	GLI family zinc finger 4	NM_138465	-0.67	4.11E-03
*PDGFRL***	Platelet derived growth factor receptor like	NM_006207	-0.69	3.61E-04
GAPDHS	Glyceraldehyde-3-phosphate dehydrogenase. spermatogenic	NM_014364	-0.71	6.62E-03
ATP6V0E2	ATPase H + transporting V0 subunit e2	NM_145230 NM_001289990 NM_001100592	-0.71 -0.74 -0.76	5.71E-04 4.08E-04 1.75E-04
*TNFRSF6B***	TNF receptor superfamily member 6b	NM_003823	-0.86	3.96E-03
PTPRQ	Protein tyrosine phosphatase. receptor type Q	NM_001145026	-0.94	4.14E-03

Table 6. DETs in co-cultured Adipo $_{HG-> LG}$*vs* Adipo $_{HG-> LG}$ UP-regulated in Co-Cultured Adipo $_{HG-> LG}$vs. Co-Cultured Adipo $_{HG}$; ** DW-regulated in Co-Cultured Adipo $_{HG-> LG}$vs. Co-Cultured Adipo $_{HG}$.

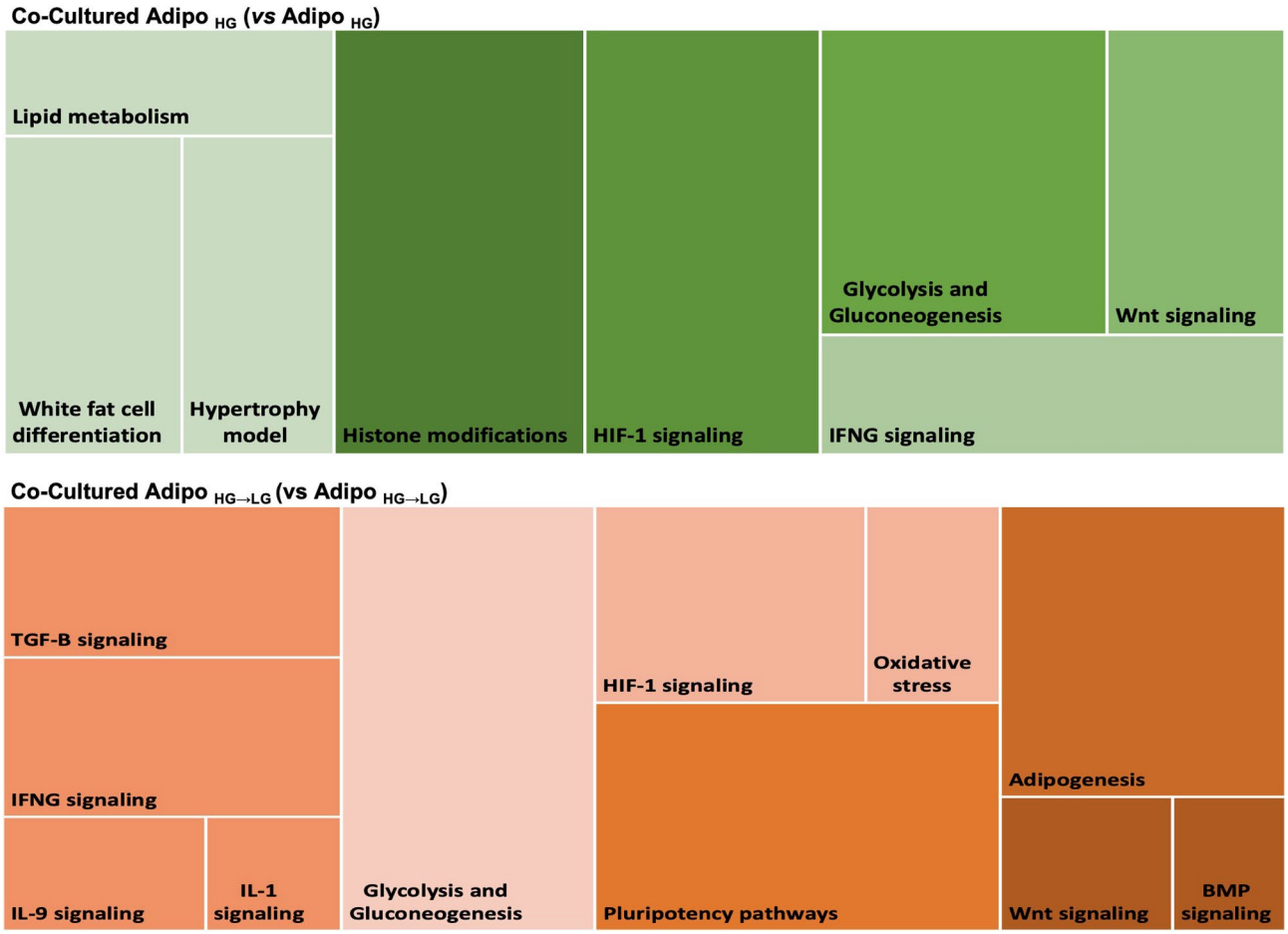

Figure 8. Pathway analysis of DEGs in adipocytes. Selected processes (Z-score > 1.5) from pathway enrichment of DEGs (p-val < 0.05) in Co-Cultured Adipo HG (*vs* Adipo HG) and Co-Cultured Adipo HG-> LG (*vs* Adipo HG-> LG). Color grading groups related processes. The size of each square reflects the number of DEGs involved in the process.

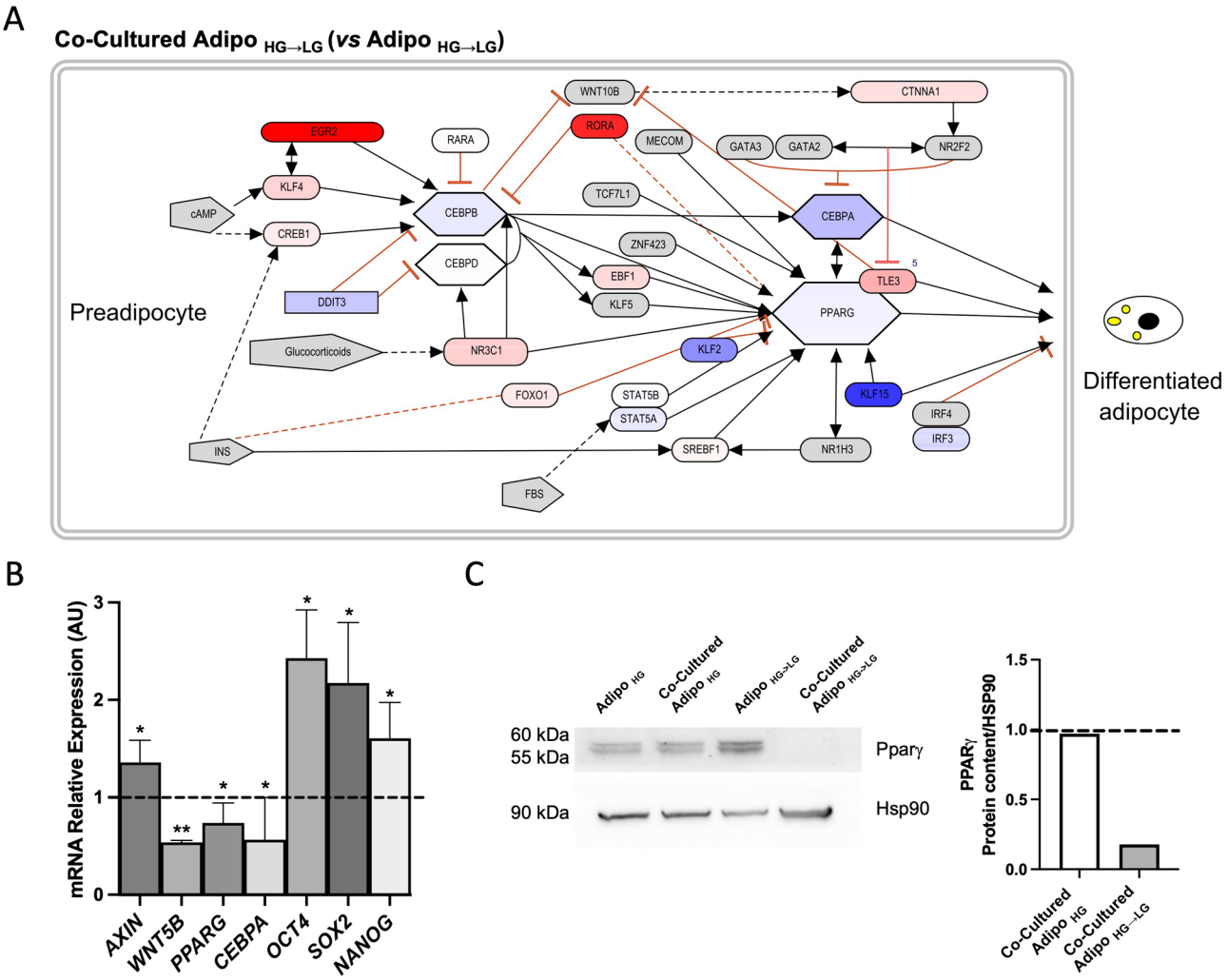

Figure 9. Glucose-modulated adipogenic and multipotency markers in adipocytes co-cultured with BC cells. Adipocytes were co-cultured with MCF7 (4 days) while exposed to basal 25mM (Co-Cultured Adipo $_{HG}$) or shifted to 5.5mM (Co-Cultured Adipo $_{HG->LG}$) glucose. **A**) Representative images of adipogenic process in Co-Cultured Adipo $_{HG->LG}$ (*vs* monocultured MCF7 $_{HG->LG}$). Red color indicates UP-regulated genes; blue color indicates DW-regulated genes (p-val<0.05). **B**) mRNA expression levels of pluripotency and self-renewal markers. Data were normalized on the peptidyl prolyl cis-trans isomerase A (*PPIA*) gene as internal standard. Results were represented as bar graph of 3–5 independent triplicate experiments showing mRNA levels in Co-Cultured Adipo $_{HG->LG}$ as relative expression (2−ΔΔCt) compared to that in monocultured Adipo $_{HG->LG}$ (control cells, dotted line). * denotes statistically significant values compared with monocultured cells (*p-val<0.05).C) Representative Western blot showing PPARγ protein levels in Co-Cultured or mono-cultured Adipo $_{HG/HG->LG.}$ Hsp90 was used as loading control. Bar graphs show the relative quantification (pixel density analysis) of protein levels in Co-Cultured Adipo $_{HG}$ and Co-Cultured Adipo $_{HG->LG}$ compared to that in monocultured Adipo $_{HG}$ and Adipo $_{HG->LG}$, respectively (dotted line). See Supplementary Figure S1-B.

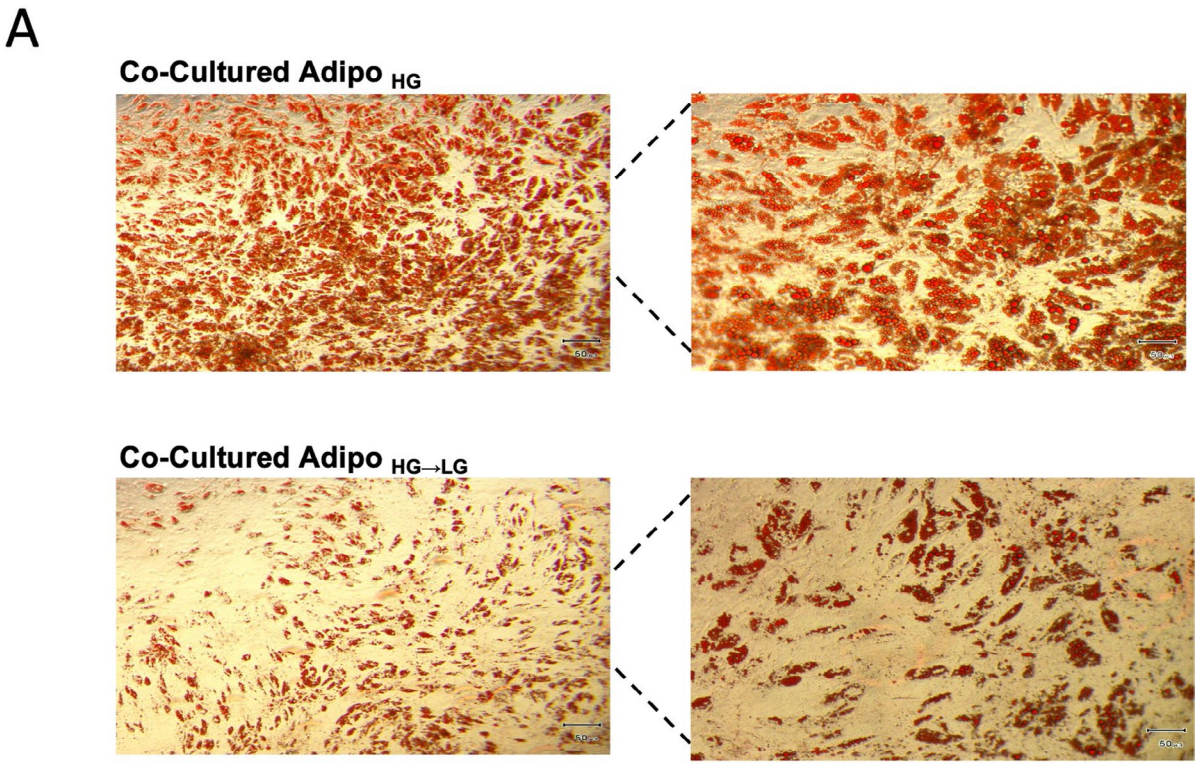

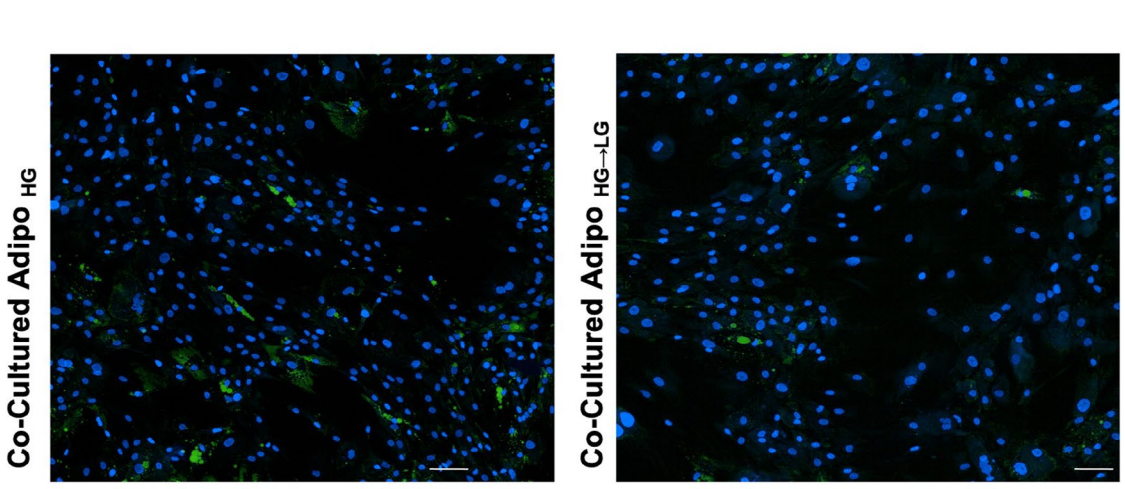

	% Bodipy Positive Cells	Mean of LD/Cells	Total LD area/Cells
Co-Cultured Adipo $_{HG}$	40.42	1.93	2.29
Co-Cultured Adipo $_{HG→LG}$	33.71	1.49	1.95
Co-Cultured Adipo $_{HG}$	55.21	1.97	2.13
Co-Cultured Adipo $_{HG→LG}$	39.11	0.86	1.37

Figure 10. Effect of BC cells onto lipid accumulation in adipocyte exposed to different glucose environment. Co-Cultured Adipo $_{HG}$ and Co-Cultured Adipo $_{HG-> LG}$ were stained for quantification of lipid droplets (LD). (**A**) Representative images from Oil Red O staining (4X and 10X magnification; scale bars 50 μm); (**B**) Representative confocal microscopy images (10X magnification; scale bars 100 μm); adipocyte differentiation grade was quantified by considering the number of Bodipy positive cells, the number of Bodipy spots (LD) and the total Bodipy area (LD area) respect to the total number of cells.

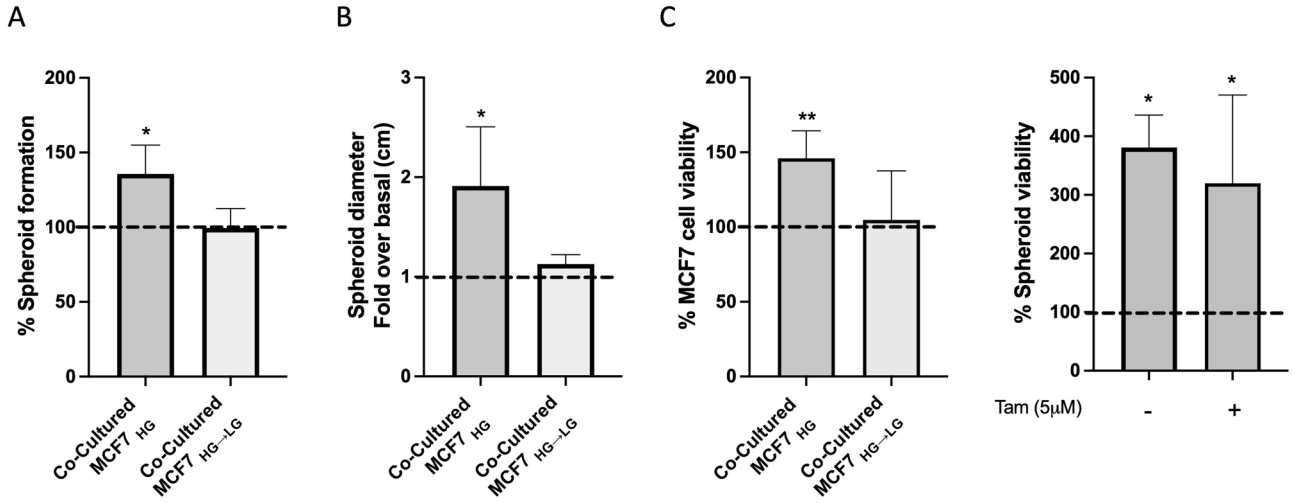

Figure 11. Effect of glucose and adipocytes on BC cell phenotype. MCF7 and adipocytes were co-cultured (4 days) while exposed to basal 25mM or shifted to 5.5mM glucose (Co-culture $_{HG}$ or Co-culture $_{HG-> LG,}$ respectively). (**A**) Conditioned media from Co-culture $_{HG}$ or Co-culture $_{HG-> LG}$ were used to set up three-dimensional cultures of MCF7 from Co-culture $_{HG}$ or Co-culture $_{HG-> LG,}$ respectively. As control, three-dimensional cultures were obtained from mono-cultured MCF7 while exposed to HG or HG-> LG medium. After 10 days, mammosphere number and diameter were obtained (see Methods). Bars represent mean ± SD of 4 independent experiments and show the percentage of mammosphere formation/fold over basal in MCF7 from Co-culture $_{HG}$ or Co-culture $_{HG-> LG}$ compared to monocultured MCF7 $_{HG}$ or MCF7 $_{HG-> LG,}$ respectively (dotted line). (**B**) Co-Cultured and monocultured MCF7 $_{HG}$ or $_{HG-> LG}$ were treated with Tamoxifen (5μM). After 72 h, cell viability was assessed by sulforhodamine B assay (see Methods). Data represent the mean ± SD of at least three independent triplicate experiments showing the percentage of viable Co-Cultured MCF7 $_{HG}$ or $_{HG-> LG}$ compared to Mono-Cultured MCF7 $_{HG}$ or $_{HG-> LG}$, respectively (100% viability, dotted line). (**C**) Mammospheres obtained from co-cultured or monocultured MCF7 were treated with Tamoxifen (5μM) while exposed to HG conditioned - or not - medium. After 72 h, cell viability was assessed (see Methods). As control, cell viability of untreated spheroids from co-cultures or monocultures in HG was also measured. Data represent the mean ± SD of 4 independent experiments and show the percentage of spheroid viability of MCF7 from co-cultures in absence or in presence of Tamoxifen, compared to those from mono-cultures (100% viability, dotted lines). A-B-C). * denotes statistically significant values compared monocultures (* $p$val < 0.05; ** pval < 0.01).

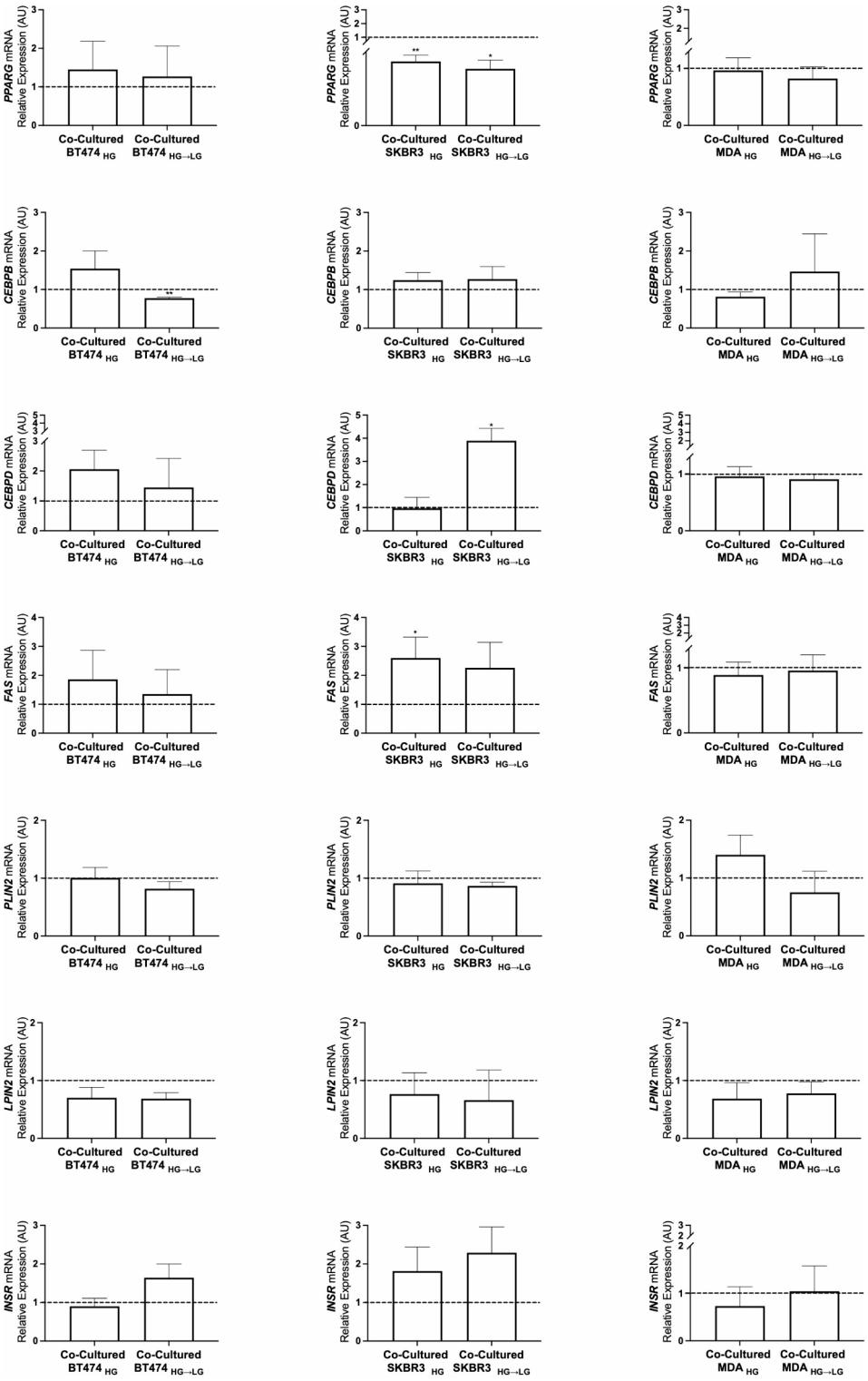

Figure 12. Glucose-modulated adipogenic markers in BC cell lines co-cultured with adipocytes. BT474 (ER^+ HER^+ PR^-), SKBR3 (ER^- HER^+ PR^-) and MDA-MB231 (ER^- HER^- PR^-) BC cells were co-cultured with adipocytes while exposed to basal 25mM (Co-Cultured BT474/SKBR3/MDA-MB231 $_{HG}$) or shifted to 5.5mM (Co-Cultured BT474/SKBR3/MDA-MB231 $_{HG-> LG}$) glucose. After 4 days, mRNA expression levels of adipogenesis-related markers were analyzed. Data were normalized on the Ribosomal Protein S2 (*RPS23*) gene as internal standard. Results were represented as bar graph of 3–4 independent triplicate experiments showing mRNA levels in Co-Cultured BT474/SKBR3/MDA-MB231 $_{HG}$ and Co-Cultured BT474/SKBR3/MDA-MB231 $_{HG-> LG}$ as relative expression ($2-\Delta\Delta Ct$) compared to that in monocultured BT474/SKBR3/MDA-MB231 $_{HG}$ and BT474/SKBR3/MDA-MB231 $_{HG-> LG}$, respectively (control cells, dotted line). * denotes statistically significant values compared with monocultured cells (* p-val < 0.05; ** p-val < 0.01).

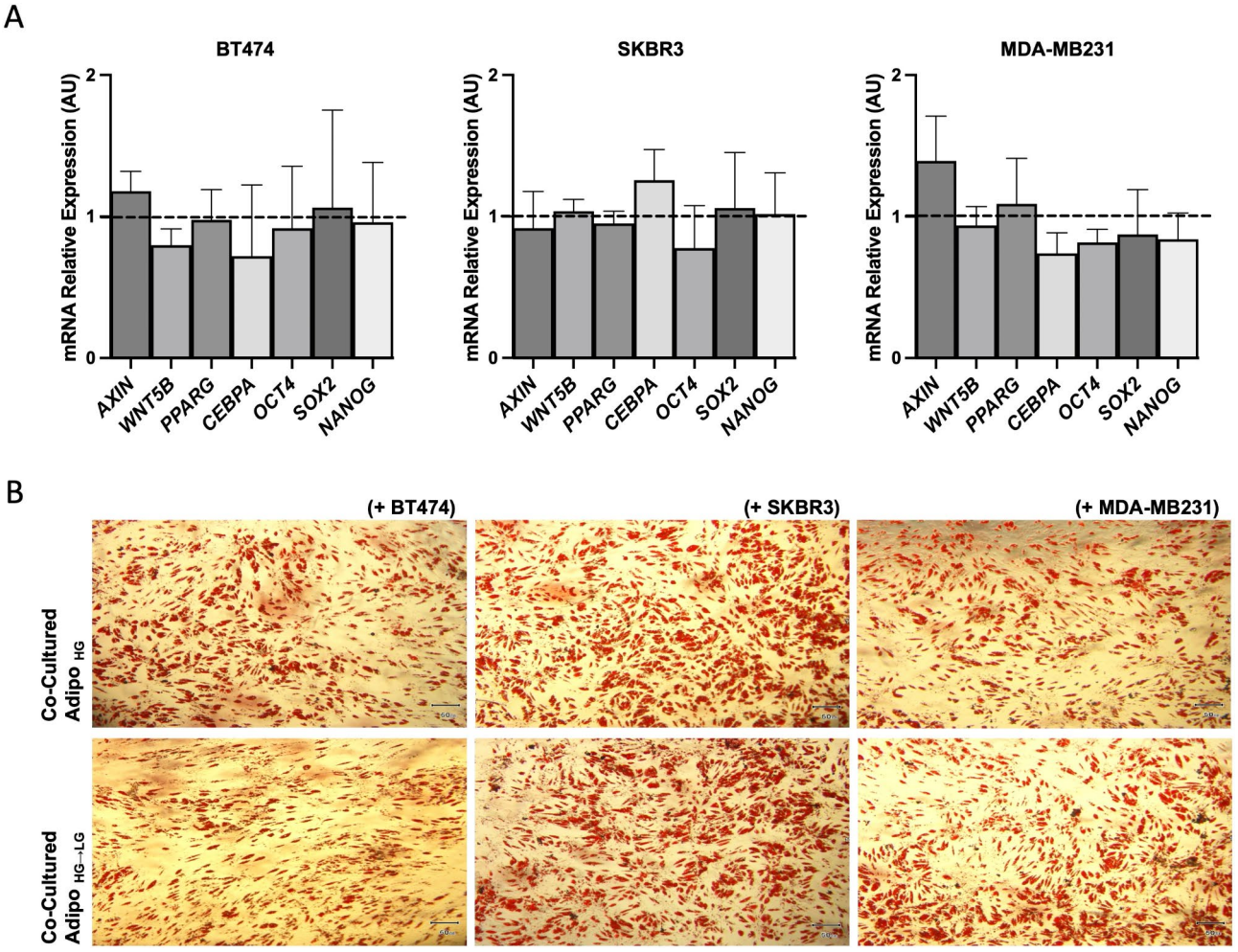

Figure 13. Glucose-modulated adipogenic and multipotency markers in adipocytes co-cultured with BC cell lines. Adipocytes were co-cultured (4 days) with BT474 (ER^+ HER^+ PR^-), SKBR3 (ER^- HER^+ PR^-) and MDA-MB231 (ER^- HER^- PR^-) BC cells while exposed to basal 25mM (Co-Cultured Adipo $_{HG}$) or shifted to 5.5mM (Co-Cultured Adipo $_{HG-> LG}$) glucose. (**A**) mRNA expression levels of pluripotency and self-renewal markers were measured. Data were normalized on the peptidyl prolyl cis-trans isomerase A (*PPIA*) gene as internal standard. Results were represented as bar graph of 3–5 independent triplicate experiments showing mRNA levels in Co-Cultured Adipo $_{HG-> LG}$ as relative expression ($2-\Delta\Delta Ct$) compared to that in monocultured Adipo $_{HG-> LG}$ (dotted line). (**B**) Co-Cultured Adipo $_{HG}$ and Co-Cultured Adipo $_{HG-> LG}$ were stained for quantification of lipid droplets (LD). Representative images from Oil Red O staining (10X magnification; scale bars 50 μm);.

Data availability

Sequence data that support the findings of this study have been deposited in the NCBI Gene Expression Omnibus repository with GEO accession number GSE243555 (temporary reviewer access token: "mdabmeyehrgxrul").

Received: 13 March 2024; Accepted: 15 October 2024
Published online: 21 October 2024

References

1. Rahman, I., Athar, M. T. & Islam, M. Type 2 diabetes, obesity, and Cancer Share some Common and critical pathways. *Front. Oncol.***10**, 600824 (2021).
2. Scully, T., Ettela, A., LeRoith, D., Gallagher, E. J. & Obesity Type 2 diabetes, and Cancer Risk. *Front. Oncol.***10**, 615375 (2021).
3. Smolarz, B., Nowak, A. Z. & Romanowicz, H. Breast Cancer-epidemiology, classification, Pathogenesis and treatment (review of literature). *Cancers (Basel)*. **14**, 2569 (2022).
4. Panigrahi, G. *et al.* Diabetes-associated breast cancer is molecularly distinct and shows a DNA damage repair deficiency. *JCI Insight*. **8**, e170105 (2023).
5. Devericks, E. N., Carson, M. S., McCullough, L. E., Coleman, M. F. & Hursting, S. D. The obesity-breast cancer link: a multidisciplinary perspective. *Cancer Metastasis Rev.***41**, 607–625 (2022).

6. Balaban, S. *et al*. Adipocyte lipolysis links obesity to breast cancer growth: adipocyte-derived fatty acids drive breast cancer cell proliferation and migration. *Cancer Metab.***5**, 1 (2017).
7. Warburg, O. On the origin of cancer cells. *Science*. **123**, 309–314 (1956).
8. Yang, K. *et al*. The role of lipid metabolic reprogramming in tumor microenvironment. *Theranostics*. **13**, 1774–1808 (2023).
9. Schiliro, C. & Firestein, B. L. Mechanisms of metabolic reprogramming in Cancer cells supporting enhanced growth and proliferation. *Cells*. **10**, 1056 (2022).
10. Hoy, A. J., Balaban, S. & Saunders, D. N. Adipocyte-tumor cell metabolic crosstalk in breast Cancer. *Trends Mol. Med.***23**, 381–392 (2017).
11. Rybinska, I., Agresti, R., Trapani, A., Tagliabue, E. & Triulzi, T. *Adipocytes Breast Cancer Thick Thin Cells***9**, 560 (2020).
12. Hanahan, D. & Weinberg, R. A. Hallmarks of cancer: the next generation. *Cell*. **144**, 646–674 (2011).
13. Kim, D. S., Scherer, P. E. & Obesity Diabetes, and increased Cancer progression. *Diabetes Metab. J.***45**, 799–812 (2021).
14. Ambrosio, M. R. *et al*. Glucose enhances pro-tumorigenic functions of mammary adipose-derived mesenchymal Stromal/Stem cells on breast Cancer cell lines. *Cancers (Basel)*. **14**, 5421 (2022).
15. Wu, Q. *et al*. Cancer-associated adipocytes: key players in breast cancer progression. *J. Hematol. Oncol.***12**, 95 (2019).
16. D'Esposito, V. *et al*. Mammary adipose tissue control of breast Cancer progression: impact of obesity and diabetes. *Front. Oncol.***10**, 1554 (2020).
17. Zhao, C. *et al*. Cancer- associated adipocytes: emerging supporters in breast cancer. *J. Exp. Clin. Cancer Res.***39**, 156 (2020).
18. Rybinska, I., Mangano, N., Tagliabue, E. & Triulzi, T. Cancer-Associated adipocytes in breast Cancer: causes and consequences. *Int. J. Mol. Sci.***22**, 3775 (2021).
19. Choi, J., Cha, Y. J. & Koo, J. S. Adipocyte biology in breast cancer: from silent bystander to active facilitator. *Prog Lipid Res.***69**, 11–20 (2018).
20. D'Esposito, V. *et al*. Adipocyte-released insulin- like growth factor-1 is regulated by glucose and fatty acids and controls breast cancer cell growth in vitro. *Diabetologia*. **55**, 2811–2822 (2012).
21. D'Esposito, V. *et al*. Adipose microenvironment promotes triple negative breast cancer cell invasiveness and dissemination by producing CCL5. *Oncotarget*. **7**, 24495–24509 (2016).
22. Ambrosio, M. R. *et al*. Glucose impairs tamoxifen responsiveness modulating connective tissue growth factor in breast cancer cells. *Oncotarget*. **8**, 109000–109017 (2017).
23. Arneth, B. Tumor Microenvironment. *Med. (Kaunas)*. **56**, 15 (2019).
24. Turner, K. M., Yeo, S. K., Holm, T. M., Shaughnessy, E. & Guan, J. L. Heterogeneity within molecular subtypes of breast cancer. *Am. J. Physiol. Cell. Physiol.***1**, C343–C354 (2021).
25. Pati, S., Irfan, W., Jameel, A., Ahmed, S. & Shahid, R. K. Obesity and Cancer: a current overview of Epidemiology, Pathogenesis, outcomes, and management. *Cancers (Basel)*. **15**, 485 (2023).
26. Wang, Y. Y. *et al*. Mammary adipocytes stimulate breast cancer invasion through metabolic remodeling of tumor cells. *JCI Insight*. **2**, e87489 (2017).
27. Zembroski, A. S., Andolino, C., Buhman, K. K. & Teegarden, D. Proteomic characterization of cytoplasmic lipid droplets in human metastatic breast Cancer cells. *Front. Oncol.***11**, 576326 (2021).
28. Tan, J., Buache, E., Chenard, M. P., Dali-Youcef, N. & Rio, M. C. Adipocyte is a non- trivial, dynamic partner of breast cancer cells. *Int. J. Dev. Biol.***55** (7–9), 851–859 (2011).
29. Aprile, M. *et al*. PPARγΔ5, a naturally Occurring Dominant-negative splice isoform, impairs PPARγ function and adipocyte differentiation. *Cell. Rep.***25**, 1577–1592e6 (2018).
30. Ambrosio, M. R. *et al*. Serotoninergic receptor ligands improve tamoxifen effectiveness on breast cancer cells. *BMC Cancer*. **22**, 171 (2022).
31. Dobin, A. *et al*. STAR: ultrafast universal RNA-seq aligner. *Bioinformatics*. **29**, 15–21 (2013).
32. Anders, S., Pyl, P. T. & Huber, W. HTSeq–a Python framework to work with high- throughput sequencing data. *Bioinformatics*. **31**, 166–169 (2015).
33. Love, M. I., Huber, W. & Anders, S. Moderated estimation of Fold change and dispersion for RNA-seq data with DESeq2. *Genome Biol.***15**, 550 (2014).

Acknowledgements

We express our gratitude to Associazione Italiana per la Ricerca sul Cancro (AIRC), European Foundation for the Study of Diabetes (EFSD), University of Naples "Federico II" and Regione Campania for financing the study. We thank the Euro-BioImaging facility at the IEOS (CNR), Naples for help with microscopy experiments.

Author contributions

Conceptualization and design of the work: M.R.A. and P.F. Methodology: K.W.J.D., V.C., D.L., V.D. Data acquisition: M.R.A., T.M., S.D.P., M.P., G.M., R.B., S.C. Data analysis: M.R.A., M.E.A., T.M., S.D.P., M.P. Data interpretation: M.R.A. and P.F. Resources: F.D. and F.S. Original draft preparation: M.R.A. and M.E.A. Writing—review and editing: A.I.C.W., F.B. and P.F. Supervision and project administration: P.F. All authors reviewed the manuscript.

Funding

This research was funded by Associazione Italiana per la Ricerca sul Cancro (AIRC n.IG2023/29378 to P.F.), European Foundation for the Study of Diabetes (EFSD/Diabetes and Cancer Programme; EFSD/Lilly Research Fellowship Programme 2016/0052351 to M.R.A.), MUR (Progetti di Rilevante Interesse Nazionale – PRIN 2022 - n. 2022KTJLHL to M.R.A., n. P2022LPJM4 to P.F., Progetto "National Biodiversity Future Center - NBFC" PNRR - CN_00000033 to M.R.A.), Sostegno Territoriale Attività di Ricerca-Linea2 (STAR-L2 2017/001398 to M.R.A.), Regione Campania (POR FESR 2014–2020 – Projects COEPICA and SATIN to P.F. and F.B.).

Declarations

Ethic declarations

The study was conducted in accordance with the Declaration of Helsinki, and approved by the Ethics Committee of University of Naples "Federico II") (protocol code prot. n. 138/16, date of approval 09-06-2016).

Informed consent
Informed consent was obtained from all subjects involved in the study.

Competing interests
The authors declare no competing interests.

Additional information
Supplementary Information The online version contains supplementary material available at https://doi.org/10.1038/s41598-024-76522-7.

Correspondence and requests for materials should be addressed to M.R.A. or P.F.

Reprints and permissions information is available at www.nature.com/reprints.

Publisher's note Springer Nature remains neutral with regard to jurisdictional claims in published maps and institutional affiliations.